DOKUZ EYLÜL UNIVERSITY
GRADUATE SCHOOL OF NATURAL AND APPLIED SCIENCES

SYNTHESIS, CHARACTERIZATION AND APPLICATIONS OF FLAME RETARDANT POLYMER COMPOSITES

by
Hasibe BÖLÜK

July, 2017
İZMİR

SYNTHESIS, CHARACTERIZATION AND APPLICATIONS OF FLAME RETARDANT POLYMER COMPOSITES

A Thesis Submitted to
the Graduate School of Natural and Applied Sciences of Dokuz Eylül University
In Partial Fulfillment of the Requirements for the Degree of Doctor of Philosophy in Chemistry Program

by
Hasibe BÖLÜK

July, 2017
İZMİR

PH.D. THESIS EXAMINATION RESULT FORM

We have read the thesis entitled **"SYNTHESIS, CHARACTERIZATION AND APPLICATIONS OF FLAME RETARDANT POLYMER COMPOSITES"** completed by **HASİBE BÖLÜK** under supervision of **PROF. DR. MEHMET KADİR YURDAKOÇ** and we certify that in our opinion it is fully adequate, in scope and in quality, as a thesis for the degree of Doctor of Philosophy.

Prof. Dr. Mehmet Kadir YURDAKOÇ

Supervisor

Prof. Dr. Mustafa Yavuz ERGÜN

Thesis Committee Member

Assist. Prof. Dr. Aylin ZİYLAN

Thesis Committee Member

Prof. Dr. Mehmet BALCAN

Examining Committee Member

Prof. Dr. Ahmet AKBAŞ

Examining Committee Member

Prof.Dr. Emine İlknur CÖCEN
Director
Graduate School of Natural and Applied Sciences

ACKNOWLEDGEMENTS

First of all, I would like to express my deep sense of gratitude to my advisor Prof. Dr. Mehmet Kadir YURDAKOÇ for his constructive ideas, help, constant support, guidance and contributions during my PhD research. I would also like to thank my committee members, Prof. Dr. Yavuz ERGUN and Assist. Prof. Dr. Aylin ZİYLAN for reviewing my work and offering valuable suggestions and sharing their visions about the content of my thesis.

I would like to thank to Dr. Aylin ALTINIŞIK TAĞAÇ for her assistance and friendship. I would also like to express my genuine gratitude to each of people, although it would be impossible for me to name all.

I would like to thank Dr. Hüseyin AL, Eko Boya for industrial applications of coatings using nanotechnological methods for supporting during this study. I would like also thank to Prof. Dr. Cahit HELVACI and Berk ÇAKMAKOĞLU, Likya Minelco Madencilik Sti. and Minelco Specialities Limited for supplying the Huntite samples. I would like to thank Prof. Dr. Erdal ÇELİK for his help for the DTA and LOI-UL94 Lab facilities. I thank to our students Yağmur Oruç and Elif Yılmaz for their kind contribution by doing UL94 Experiments in our Laboratories.

A special thank goes to my family for their concern, confidence and support. Finally, I extend my greatest thanks to my husband Behçet Kağan BÖLÜK and my lovely son Baybars BÖLÜK who unconditionally supported me. The successful completion of this study would not have been possible without their constant love and encouragement.

Hasibe BÖLÜK

SYNTHESIS, CHARACTERIZATION AND APPLICATIONS OF FLAME RETARDANT POLYMER COMPOSITES

ABSTRACT

In this study, flame retardant properties of Huntite, Magnesium carbonate hydroxy hydrate (MCHH) in polymer composite coating materials were investigated and developed in some respect. For these reasons, polymer composites were obtained by adding different amounts of environmental friendly halogen-free and flame retardant minerals such as Huntite, Magnesium carbonate hydroxy hydrate and their mixtures to polyester-epoxy hybrid resins. The synthesized polymer composite materials were then deposited onto metal plates and characterized by XRD, FT-IR, TG, DTA, DSC and SEM analysis. LOI and UL94 flammability tests were carried out to examine the possible flame retardant properties of the composite materials.

The best results were obtained in Huntite reinforced composites. Plate 4 and Plates 7, 8 and 9 showed similar behavior. Huntite does not seem to have the flame retarding feature alone. It should be used together with Barium sulphate and MCHH, but not more than totally 40 percent as filler content. Huntite and MCHH mixtures exhibited more effective flame retarding properties in accordance with the studied polymer matrix.

Keywords: Huntite, Magnesium carbonate hydroxy hydrate, flame retardant, polymer composite

ALEV GECİKTİRİCİLİ POLİMER KOMPOZİTLERİN SENTEZ, KARAKTERİZASYON VE UYGULAMALARI

ÖZ

Bu çalışmada Huntite ve Magnezyum karbonat hidroksi hidrat (MCHH) içeren polimer kompozit kaplama malzemelerinin alev geciktirme özellikleri incelenmiş ve geliştirilmeye çalışılmıştır. Bu kapsamda polyester-epoksi hibrit polimer matriks malzemelerine çevre dostu halojen içermeyen Huntit, Magnezyum karbonat hidroksi hidrat mineralleri ve bunların karışımları farklı miktarlarda ilave edilerek polimer kompozit malzemeler elde edilmiştir. Üretilen kompozit malzemelerin karakterizasyon çalışmaları; XRD, FT-IR, TG, DTA, DSC ve SEM cihazları ile yapılmıştır. Ayrıca bu polimer kompozit malzemelerin alev geciktirime özelliklerinin belirlenmesi için LOI ve UL94 yanıcılık testleri de yapılmıştır.

Huntit ile güçlendirilmiş kompozitlerle en iyi sonuçlar elde edilmiştir. Plaka 4 ile 7., 8. ve 9. Plakalar benzer davranış göstermiştir. Huntit, başlı başına çok etkili bir yangın geciktirici değildir. Huntite, Baryum sülfat ve MCHH ile birlikte ancak dolgu maddesi içeriği de toplam olarak yüzde kırk dan fazla kullanılmalıdır. Huntit ve MCHH karışımlarının, polimer matriksle uyum gösterdikleri ve alev geçiktirici özellikler sergilediği belirlenmiştir.

Anahtar Kelimeler: Huntite, Magnezyum karbonat hidroksi hidrat, alev geciktirme, polimer kompozit

CONTENTS **Page**

Ph.D. THESIS EXAMINATION RESULT FORM ii
ACKNOWLEDGEMENTS iii
ABSTRACT iv
ÖZ v
LIST OF FIGURES viii
LIST OF TABLES x

CHAPTER ONE - INTRODUCTION .....

1.1 Flame Retardants 1
1.2 Flame Retardant Materials and Mechanisms 5
1.2.1 Halogens 7
1.2.2 Borates 8
1.2.3 Phosphorus 9
1.2.4 Silicon 10
1.2.5 Nitrogen 10
1.2.6 Metal Hydroxide and Carbonate Fire Retardants 10
1.2.6.1 Aluminum Hydroxide 13
1.2.6.2 Magnesium Hydroxide 14
1.2.6.3 Huntite and Hydromagnesite 16
1.2.7 Synergism 21
1.2.8 Criteria for Selection of Flame Retardants 21
1.3 Nanocomposites 22
1.4 Fire Tests and Standards 23
1.4.1 Limited Oxygen Index (LOI) 23
1.4.2 UL 94 Vertical Test 25
1.5 Powder Coating 27
1.5.1 Types of Powder Coating 29
1.5.2 Powder Coating Formulations 30
1.5.2.1 Fillers 31

1.5.2.1.1 Barium Sulphate. 31
1.5.3 Producing Industrial Powder Coatings 32
1.5.4 The Powder Coating Application 32
1.6 The Aim of the Thesis 33

CHAPTER TWO - MATERIALS AND METHODS 36

2.1 Materials 36
2.1.1 Preparation of Polymer Composite Coatings 36
2.2 Fourier Transform Infrared Spectroscopy (FTIR) Analysis 38
2.3 X-Ray Diffraction Analysis (XRD) 38
2.4 ThermalAnalysis 39
2.5 Scanning Electron Microscopy (SEM) 39
2.6 Flame Retardancy Tests (LOI and UL94 Tests) 39

CHAPTER THREE - RESULTS AND DISCUSSION 43

3.1 X-Ray Diffraction (XRD) Analysis 43
3.2 Scanning Electron Microscopy (SEM) Analysis 49
3.3 Fourier Transform Infrared Spectroscopy (FTIR) analysis 53
3.4 Thermogravimetric Analysis (TGA) 56
3.5 Differential Thermal Analysis 62
3.6 Differential Scanning Calorimetric (DSC) Analysis 63
3.7 UL94 Flammability Test 65

CHAPTER FOUR - CONCLUSIONS 68

REFERENCES 69

LIST OF FIGURES

Page

Figure 1.1 Fire Triangle 3

Figure 1.2 Thermogravimetry of ATH and $Mg(OH)_2$ 12

Figure 1.3 Differential scanning calorimetry of ATH and $Mg(OH)_2$ 12

Figure 1.4 Smoke emissions from polypropylene composites 13

Figure 1.5 SEM Images of Huntite particles 18

Figure 1.6 TGA profile of natural Hydromagnesite, Huntite and a 60:40 mixture of Hydromagnesite and Huntite 19

Figure 1.7 Experimental Set-up for LOI measurement 24

Figure 1.8 Experimental Setup for UL94 Vertical Test 26

Figure 1.9 Schematic presentation of the aim of the Thesis 35

Figure 2.1 Preparation of polymer composite coatings 37

Figure 2.2 LOI Apparatus 40

Figure 2.3 UL94 Vertical Test Setup 41

Figure 2.4 UL94 Horizontal Test Setup 41

Figure 2.5 ZLT-ZY2 Needle-Flame Tester 42

Figure 3.1 XRD patterns of Huntite 44

Figure 3.2 XRD patterns of Barium Sulfate 45

Figure 3.3 XRD patterns of MCHH 46

Figure 3.4 XRD Patterns of $BaSO_4$ and Plate 0 46

Figure 3.5 XRD Patterns of Huntite and Plate 47

Figure 3.6 XRD Patterns of MCHH and Plate 7 48

Figure 3.7 XRD Patterns of Huntite and Plate 0, 1, 2 and 4 48

Figure 3.8 XRD Patterns of Huntite and Plate 0, 8 and 9 49

Figure 3.9 SEM Image of Huntite (3000×) 50

Figure 3.10 SEM Image of Basic magnesium carbonate (1000×) 51

Figure 3.11 SEM Images of Filler26-Barium sulphate ($BaSO_4$) (2500×) 51

Figure 3.12 SEM images of (a) Plate 0 (5000×), (b) Plate 1 (5000×), (c) Plate 2 (500×) (d) Plate 3 (5000×), (e) Plate 4 (5000×), (f) Plate 5 (10000×), (g) Plate 6 (2500×), (h) Plate 7 (5000×), (i) Plate 8 (2500×), (j) Plate 9 (5000×) 52-53

Figure 3.13 FTIR Spectrum of $BaSO_4$ 53
Figure 3.14 FTIR Spectrum of MCHH 55
Figure 3.15 FTIR spectra of a) Plate 0 b) Plate 1 c) Plate 2 d) Plate 3 e) Plates 4 56
Figure 3.16 TG/DTG profile of Huntite 57
Figure 3.17 TG/DTG profile of Filler26- $BaSO_4$ 58
Figure 3.18 TG/DTG profile of MCHH 58
Figure 3.19 Thermogravimetric and DTG curves of Epoxy GS 7351, Polyester 4783 and Polyester 6400 59
Figure 3.20 TGA Thermograms of the Plates 64
Figure 3.21 DSC curves of UCP 0 and UCP 4 64
Figure 3.22 UL94 Vertical Flammability Test Images of samples 67

LIST OF TABLES

Page

Table 1.1 Mineral fire retardants and their decomposition temperatures 5
Table 1.2 Formulas and properties o f Huntite & hydromagnesite..... 17
Table 1.3 LOI, flash- and self-ignition temperatures of selected polymers..... 25
Table 1.4 UL 94 flammability test classification of the materials 27
Table 2.1 Sample code and composition of the composite samples as weight %. 38
Table 3.1 TG/DTG Analysis Data of Huntite, $BaSO_4$ and MCHH 58
Table 3.2 TG/DTG Data of Epoxy GS 7351, Polyester 4783 and Polyester 6400 59
Table 3.3 TGA/DTGdata of the Plates..... 60
Table 3.4 Results of Differential Thermal Analysis for Plate 0-9. 63
Table 3.5 DSC data of the UCP 0-7 samples..... 64
Table 3.6 Formulations and Flame Retardancy for the coatings 66

CHAPTER ONE
INTRODUCTION

1.1 Flame Retardants

For centuries, humanity has been studying and exploring fire, flame, and protection from it. Heat, power and controlled use have always been a research area. In the controlled form, it would be beneficial to bring heat and power together. Otherwise, it is clearly dangerous in terms of its results. For these reasons, the study of fire and how to control and prevent unwanted fires are of great importance. Fuel, Heat and Oxygen are required to burn any combustible materials.

Each year, thousands of people die in fires, tens of thousands of people are wounded and large financial losses occur. With developments in technology, industry, and with increasing energy consumption and population, fire risks and associated financial and intangible losses increase in case of fire.

A fire is a disaster with flames getting out of control, and gain damaging characteristics. The damages caused by fires vary according to the causes of fire, their places, and the time spent to intervene. Self extinguishing of fires without any intervention is only possible when there is nothing left to burn. That is why; the fires should be intervened, in order to minimize their effects and damages.

In many application areas, it is not possible to control the potential fire risks and cannot be ruled out. Therefore products should be protected against fire possibility. The common question is how to protect against fire attacks and what level will be used. Flame retardant materials play an important role in this aspect. The global flame retardant market size was valued at USD 6.29 billion in 2015.

The report **"Flame Retardant Market by Type (ATH, Antimony Oxide, Brominated, Chlorinated, Phosphorous), Application (Epoxy, Polyolefins), and End-use Industry (Building & Construction, Electronics & Appliances, Wire & Cables, Automotive) - Global Forecast to 2021"**, The global flame retardants market

is projected to reach USD 12.81 Billion by 2021 at a CAGR of 6.4% between 2016 and 2021. The market is majorly driven by growth of the end-use industries and increasing fire safety regulations (Kandelbauer, Tondi, & Goodman, 2013; Vojta, et al., 2017; Langfeld, et al., 2015).

In order to reduce the combustibility of the polymers and to prevent the smoke or toxic fume products, the usage of flame retardants, development and applications of new fire protective materials would be necessary (Demirel, Pamuk, & Dilsiz, 2010). Flame retardancy is required not only for industries related with construction, electrical, and electronics and transport but also human demanded materials (Innes, 1996; Nelson, 1994). It is essential that new flame retardant systems are developed to meet the constantly changing demand of new regulations, standards, and test methods (Troitzsch, 1998).

A flame retardant should inhibit or even suppress the combustion process (Lu, & Hamerton, 2002). Depending on their nature, flame retardants can act chemically and/or physically in the solid, liquid, or gas phase (Nelson, 1994). They interfere with combustion during a particular stage e.g. heating, decomposition, ignition, or flame spread (Troitzsch, 1998). Although, halogens are the most widely applied flame retardant materials in the area for polymers and hybrid organic materials or in electronic devices, they do have clear disadvantages due to their toxicity during combustion (Ellis, 1993). Figure 1.1 depicts Fire Triangle.

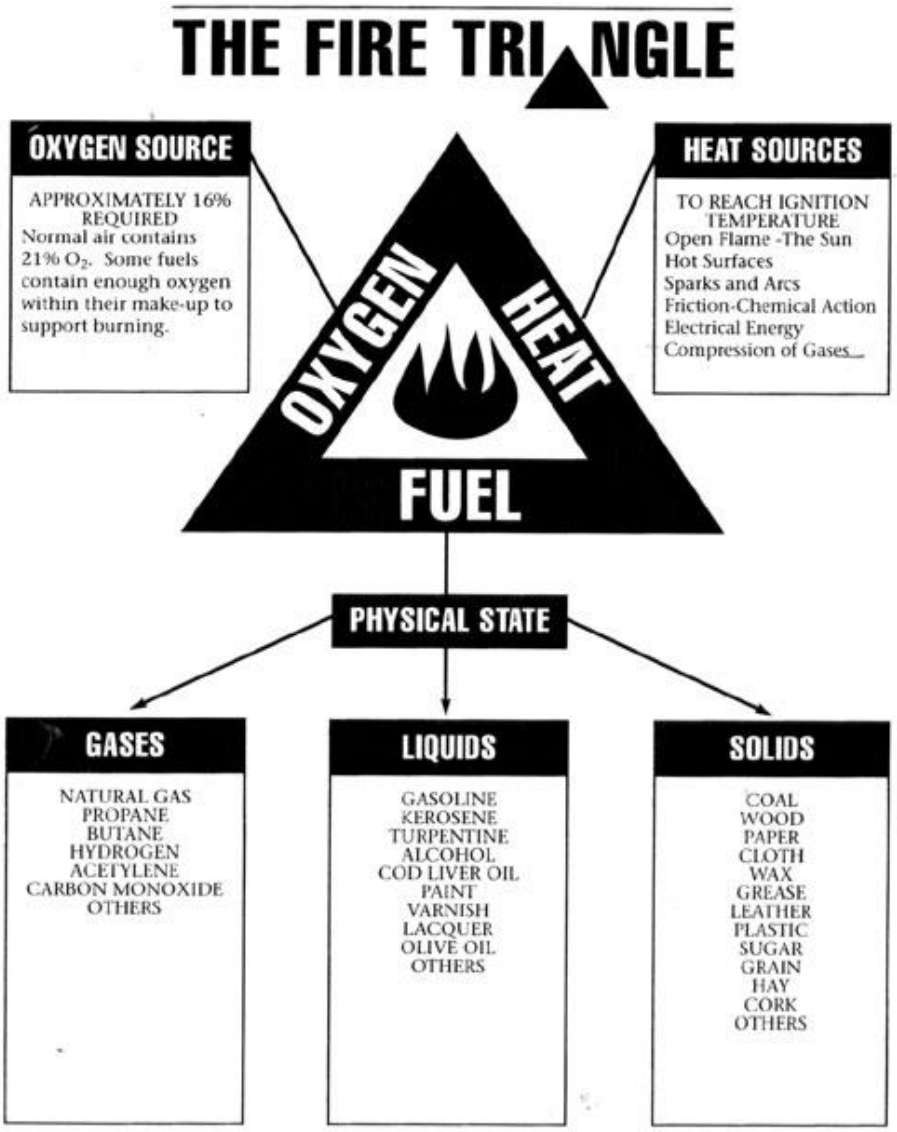


Figure 1.1 Fire Triangle (Fire triangle,http://firextinguishing.blogspot.com/search/label/Introduction, 2011)

For many years, minerals have been used in a wide variety of polymer applications. They have also been widely regarded as cost reducers and/or fillers. Minerals are often used for the flame retardancy properties for these applications. In this case, enhancements bring to polymer applications. These application properties are closely related to the physical properties of the mineral itself. Thus, in the formulation (compounding) of polymers prior to the conversion of the raw material to the finished it, ancillary materials are added that impart to the compound the required properties

of; flowability of the melt, tensile strength, bending strength, resistance to breakage by impact, resistance to the effects of oxygen or UV light, resistance to fire, suppression of smoke in the event of ultimate burning (Mureinik, 1997).

The halogenated flame retardants can be seen in many related areas in the markets. Nevertheless, those flame retardants are under pressure because of their significant disadvantages related to the formation of smoke, toxic and corrosive decomposition products. In contrast, mineral flame retardants provide in part extremely low smoke values; they absorb toxic and corrosive gases, and generate nothing but water, carbon dioxide, and harmless metal oxides. Wherever technical solutions are developed that allow the use of mineral flame retardants those formulations are preferred in many applications.

The metal hydroxides such as Aluminum hydroxide (ATH) and Magnesium hydroxide (MH) are the largest groups of mineral fire retardants that are widely used (Bolger, 1996). The fire retardant mechanism is releasing of water vapor through an endothermic decomposition leaving a thermally stable inorganic residue. When we use these metal hydroxides as fillers in polymer composites, they dilute the combustible polymer decomposition products due to water formation and cooling the condensed phase through the endothermic dehydration. In recent years, the demands for less flammable polymers in the industry have changed from ignition suppression to lower smoke and toxicity, to “halogen-free” polymer composites. In the near future, sustainable fire retarded materials will be greatly required (Hull, 2016). Mineral fire retardants and their decomposition temperatures can be summarized as in Table 1.1.

Table 1.1 Mineral fire retardants and their decomposition temperatures (Rothon, 2003)

Mineral	Chemical Formula	Approximate onset of Decomposition Temperatures (°C)
Nesquehonite	$MgCO_3.3H_2O$	70-100
Gypsum	$CaSO_4.2H_2O$	60-130
Magnesium phosphate octahydrate	$Mg_3(PO)_4.8H_2O$	140-150
Aluminum hydroxide	$Al(OH)_3$	180-200
Hydromagnesite	$Mg_5(CO_3)_4(OH)_2.4H_2O$	220-240
Dawsonite	$NaAl(OH)_2CO_3$	240-260
Magnesium hydroxide	$Mg(OH)_2$	300-320
Magnesium carbonate subhydrate	$MgO.CO_2(_{0.96})H_2O_{(0.3)}$	340-350
Boehmite	AlO[OH]	340-350
Calcium hydroxide	$Ca(OH)_2$	430-450

1.2 Flame Retardant Materials and Mechanisms

Flame retardant term is used for any materials that allow a polymer to retard or prevent a flame, or for any polymer that shows the ability to slow fire growth when ignited. In the terminology, this does not mean non-combustible or ignition resistant. These are very different terms and should not be used to define a flame-retardant material. A material that is truly non-combustible or ignition resistant either cannot be combusted or cannot be ignited with a particular size flame/heat source. A material could be flame retarded so that under a test that measures aspects of ignition or combustibility, the material is evaluated to be non-combustible/ignition resistant, but under another set of conditions it burns easily (Charles & Alexander, 2009).

Protection against fire by the usage of the flame retardants in the polymer composites must achieve at least one of several tasks during the course of a fire. These can be stated as:

- Raising of the ignition temperature,

- Reduction of the rate of burning,
- Reduction of flame spread, and
- Reduction, if not elimination, of smoke generation (Dufton, 2003).

Flame retardants can be classified in two categories as additive and reactive. The additive flame retardants are generally incorporated during the transformation process. They do not react at this stage with the polymer but only at higher temperature, at the start of a fire. They are usually mineral fillers, hybrids or organic compounds including macromolecules. On the other hand, reactive flame retardants are usually introduced into the polymer during synthesis as monomers or precursor polymers (Laoutid, 2009).

Flame retardants differ chemically from one another. Therefore, their effect mechanisms can be organized to various classes of flame retardants. These are gas- and condensed-phase-active flame retardants. Gas-phase-active flame retardants act primarily through scavenging free radicals formed in the flame. Other flame retardants generate large amounts of non-combustible gases that can dilute the flammable gases by dissociating endothermically, and decrease the temperature by absorbing heat. In the condensed-phase mechanisms, charring is most common. It could be promoted either by chemical interaction of the flame retardant and the polymer or by physical retention in the structure. It could also be promoted by catalyts or oxidative dehydrogenation reactions. Chemical mechanisms are always accompanied by one or several other physical mechanisms such as endothermic dissociation or dilution. These can be also synergistic actions (Alexander & Charles, 2007).

Polymers are generally flammable. For this reason, usages of the different fire protective materials for reducing the fire hazards are very important. There are a variety of methods for improving the fire retardancy of a polymer. The related review papers and reports about the fire retardants used commonly today (Weil & Levchik, 2006; Weil & Levchik, 2008; Lu & Hamerton, 2002; Bolger, 1996).

The principle is to try and slow the development of the fire in the beginning by limiting at least one essential components of the fire as oxygen, fuel or heat. These are controlled or reduced through either chemical or physical means depending on the fire

retardant used. The purpose is always to reduce the severity of the fire. Usage of inert fillers causes the dilution of the polymer and reduces the fuel supply. Another way is the use of active fillers that can dilute the supply of oxygen and any combustible gases. The release of non-combustible gases is a wellknown method. These inert gases are provided through endothermic decomposition of the additive which reduces the supply of heat to the decomposing polymer. This process slows the supply of flammable decomposition products to the gas phase. The free radicals formed in the flame can be disrupted without using the halogens. This leads to lower heat generation into polymer and the medium. The surface of products can be protected through the formation of a carbonaceous char by insulating and protecting the polymer from further decomposition. Here are the commercially available fire retardants in the market and are discussed shortly below.

1.2.1 Halogens

Halogens act as active fire retardants due to the free radical reactions (Bourbigot & LeBras, 2004). The mechanism is release of hydrogen halides from the decomposition of halogen containing materials, such as PVC. Then they react with the hydrogen radicals and hydroxide radicals in the flame to form molecular hydrogen or water and a halide radical as shown in Reaction 1.1-1.2. The removal of these radicals from the flame reduces naturally the combustion rate.

$$HX + H\bullet \longrightarrow H_2 + X\bullet \quad (1.1)$$

$$HX + OH\bullet \longrightarrow H_2O + X\bullet \text{ (X = Halogens, X•=Radical)} \quad (1.2)$$

On the other hand, removal of the hydroxide radicals has a significant effect on reducing the temperature of the flame. It possibly reduces the availability of the free radical for the highly exothermic conversion of carbon monoxide to carbon dioxide in these reactions (Cullis & Hirschler, 1981).

The less reactive halide radicals regenerate the hydrogen halide by abstracting hydrogen from the polymer fragments. In addition, the loss of the halide radicals from

the polymer results in unsaturation which may act as a precursor to crosslinking and formed char.

The effectiveness of halogens increases in the order of F < Cl < Br < I. Bromine and chlorine are often used as fire retardants (Bourbigot & LeBras, 2004).

Antimony trioxide (Sb_2O_3) is not a fire retardant itself, but is known as synergist (Beard, 2007).

The function of antimony trioxide begins with the formation of antimony trihalide that acts as a trap for hydrogen and hydroxide radicals (Kandola, 2008).

The reactions of the antimony halide are shown below as Reaction 1.3-1.10 (Georlette, Simons & Costa, 2000).

$$SbX_3 + H\bullet \longrightarrow SbX_2 + HX \quad (1.3)$$

$$SbX_2 + H\bullet \longrightarrow SbX + HX \quad (1.4)$$

$$SbX + H\bullet \longrightarrow Sb + HX \quad (1.5)$$

$$Sb + O\bullet \longrightarrow SbO \quad (1.6)$$

$$Sb + OH\bullet \longrightarrow SbOH \quad (X = \text{halogen and } \bullet = \text{radicals}) \quad (1.7)$$

$$SbO + H\bullet \longrightarrow SbOH \quad (1.8)$$

$$SbOH + H\bullet \longrightarrow SbO + H_2 \quad (1.9)$$

$$SbOH + OH\bullet \longrightarrow SbO + H_2O \quad (1.10)$$

As can be seen from the above reactions, the action of antimony with a halogen is very effective for the inhibition of radicalic reactions. In fact, these resulted easily in the generation of heat within the flame.

1.2.2 Borates

The usage of borates and related boron compounds as fire retardants has been reported especially for cotton (Cullis & Hirschler, 1981). The reaction is given in Reaction 1.11.

In these reactions, boric acid and borax mixture decompose endothermically with the release of water and form a glassy residue on the surface of the substrate.

$$2H_3BO_3 \xrightarrow[130-200℃]{} 2HBO_2 + 2H_2O \xrightarrow[260-270℃]{} B_2O_3 + 2H_2O \qquad (1.11)$$

During decomposition, the mixture dissolved in water generates swelling foam. It forms a glassy melt which creates a shielding effect between the substrate and the flame. This reduces the amount of oxygen and therefore reducing the oxidation of carbon and increasing char formation (Lu & Hamerton, 2002).

Zinc borates can be used instead of antimony trioxide in halogenated systems for fire performance (Weil, 2000).

The mechanism is creating a glassy surface barrier and act as condensed phase fire retardants. In electrical applications, zinc borate is used often to improve the surface electrical properties.

Synergism with zinc borate has also been reported between both ATH and magnesium hydroxide (Weil & Levchik, 2008).

1.2.3 Phosphorus

There is various phosphorus containing fire retardants such as red phosphorus, phosphates, phosphites and other phosphorus containing polymer-like molecules (Lu & Hamerton, 2002). They increase the char yield while others show inhibition action in the gas phase (Laoutid et al., 2009).

Phosphorus affects on the polymer decomposition and favor the carbon production, but the fire retardant mechanism is still not fully explained.

1.2.4 Silicon

Small additions of silicones, silicas, silicates, organosilanes and silsesquioxanes have been reported to enhance the fire retardancy by formation of char (Laoutid et al., 2006). Radical trapping in the vapor phase is also possible in some cases (Lu & Hamerton, 2002).

On the other hand, silicone polymer, or silicon dioxide can interact with zinc borate to form borosilicate glass at the combustion of polymers at high temperatures (Kim, 2003).

This mechanism has been suggested as in mixtures of magnesium hydroxide with talc and zinc borate (Weil, 2000; Laoutid et al., 2006; Kim, 2003).

1.2.5 Nitrogen

Nitrogen containing fire retardants are used in the form of melamine variants. They can be used in the condensed phase and form crosslinked structures to promote char formation. They also release ammonia that dilutes the gas phase (Beard, 2007).

1.2.6 Metal Hydroxide and Carbonate Fire Retardants

The mineral fire retardants will be discussed more in this Thesis. They are generally in the form of metal hydroxides. Aluminum hydroxide and magnesium hydroxide are the most commonly used retardants (Fink, 2004; Bolger, 1996).

The general mechanism is releasing of water vapor though an endothermic decomposition reaction. Therefore, they cool the condensed phase and dilute the combustible products in the vapor phase. The mechanism is ended with water and inorganic residue formation. They provide a protective layer on the polymer surface.

The role of these fire retardants are in such a way that it reduces the combustible products and changes the thermal conductivity and the viscosity of the resulting material.

All these actions have an indirect incidence on the polymer's fire performance. Nevertheless, some minerals are more specifically used as flame retardants owing to their behavior at high temperature. The most commonly used mineral flame retardants are especially of aluminum and magnesium hydroxides, hydroxyl carbonates and zinc borates. These fillers have a direct physical flame retardant action. As the temperature rises, they decompose endothermically and absorb energy. The release of H_2O and CO_2 dilutes combustible gases and can promote the formation of a protective ceramic or vitreous layer on the substrate surface (Laoutid et al. 2009; Rothon, 2003; Yılmaz Atay & Çelik, 2010).

Aluminum hydroxide begins to release water at about 220℃ with an endotherm of 1.17 kJ/g. On the other hand, Magnesium hydroxide starts releasing water at about 330℃ with an endotherm of 1.356 kJ/g. TG and DSC profiles obtained on heating of Aluminum hydroxide and Magnesium hydroxide are shown in Reaction 1.12-13, respectively.

$$2Al(OH)_3 \longrightarrow Al_2O_3 + 3H_2O \quad (\Delta H{=}1.17\ kJ/g) \tag{1.12}$$

$$2Mg(OH)_2 \longrightarrow 2MgO + 2H_2O \quad (\Delta H{=}1.356\ kJ/g) \tag{1.13}$$

The fire retardant mechanism of the hydroxides is heat absorption and dilution of the flame with water vapors (Reactions1.12-13). Another proposed mechanism may be the catalytic effect of anhydrous alumina which can enhance charring. Anhydrous alumina and magnesia are white highly refractory powders. They provide heat insulation effect by reflecting the heat on the surface (Lewin & Weil, 2001). Thermogravimetric curves of ATH and $Mg(OH)_2$ were shown in Figure 1.2. DSC curves of ATH and $Mg(OH)_2$ were shown in Figure 1.3.

These inorganic hydroxides are used as insulator composites together with poly(vinyl chloride) (PVC), polyethylene, and various elastomers in wire and cables.

Decrease in the amounts of metal hydroxides in the polymeric matrix will result significant gain in physical properties such as flexibility. For this reason, usage of red phosphorus, silicones, boron compounds and clay minerals as charring agents have been explored. Surface modification of metal hydroxides with surfactants improve the physical and flame retardancy properties because of homogeneous dispersion in the composites (Alexander & Charles, 2007).

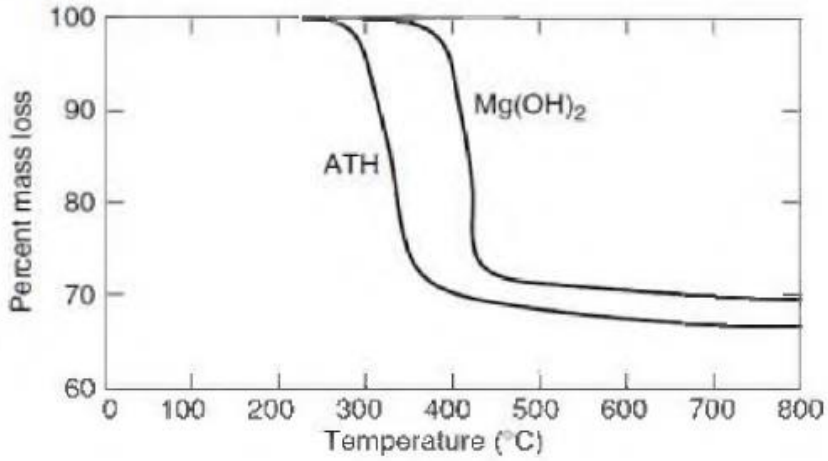


Figure 1.2 Thermogravimetry of ATH and $Mg(OH)_2$ (Alexander & Charles, 2007)

In the ATH-filled polymers, the LOI can reach values higher than 50% for EVA containing 75 weight percent of ATH and producing smoke in Figure 1.4.

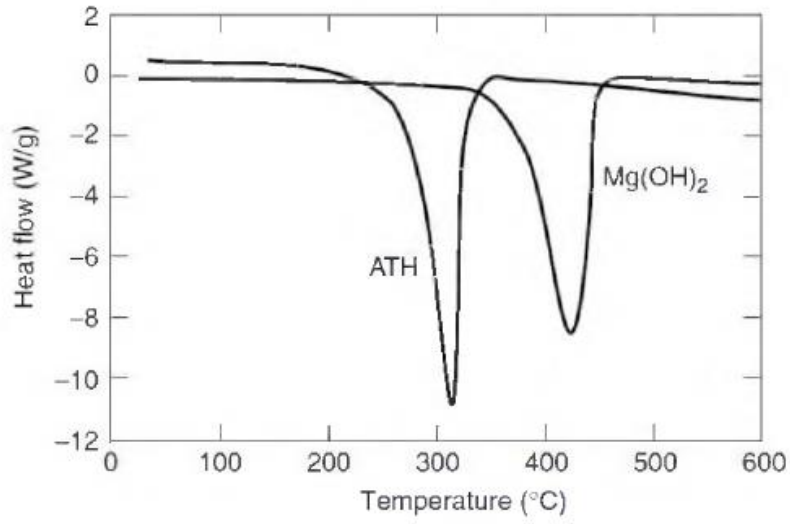


Figure 1.3 Differential scanning calorimetry of ATH and $Mg(OH)_2$ (Alexander & Charles, 2007)

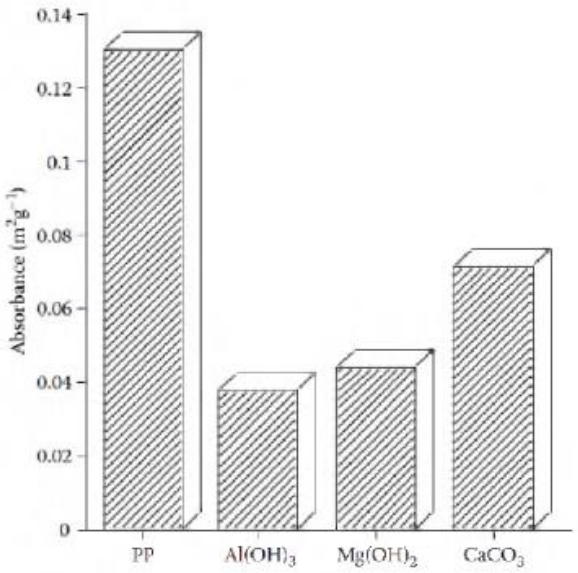


Figure 1.4 Smoke emissions from polypropylene composites (Charles & Alexander, 2009)

In several reports, smoke suppressing tendencies of the fillers have been demonstrated in various polymers such as ethylene-propylene-diene elastomers, polypropylene, polystyrene, modified polyphenylene oxide, polybutylene terephthalate, and acrylnitril butadiene styrol copolymer (ABS). As an example, Figure 1.4 illustrates smoke reductions obtained in polypropylene. Smoke reduction results from the deposition of carbon onto the high surface area oxide surface. The volatilization of carbonaceous residue as carbon oxides reduces the effects of smoke produced (Charles & Alexander, 2009).

The use of small amounts of nanosized magnesium hydroxide showed interesting fire performances (Henrist et al. 2003). LOI measured with EVA containing 50% weight percent of magnesium hydroxide increased from 24% to 38.3%. The enhancement was due to the homogeneous dispersion of the nanoparticles in EVA by leading compact and cohesive char (Yıldırım, 2013).

1.2.6.1 Aluminum Hydroxide

Aluminum hydroxide is defined by various names. These are aluminum trihydroxide, aluminum trihydrate, alumina trihydrate or simply ATH. Aluminum hydroxide is the most widely used fire retardant (Weil & Levchik 2008; Horn, 2000).

It decomposes in accordance with the reaction shown in Reaction1.14.

$$2Al(OH)_3 \longrightarrow Al_2O_3 + 3H_2O \quad (1.14)$$

On the other hand, the decomposition enthalpy of ATH is given as between 1170 and 1300 Jg^{-1} (Lewin & Weil, 2001; Horn, 2000; Hancock & Rothon, 2003; Rothon, 2003).

The mass loss of ATH is approximately 35 percent as water vapor through endothermic decomposition. The decomposition reaction starts to occur at about 180-200 ℃ (Rothon, 2003). This decomposition temperature limits the usage of ATH at elevated temperatures. It cannot be used in polymers that are processed at or above this temperature.

High loading levels as 60% by weight of ATH are usually required in order to achieve good fire retardant properties (Weil & Levchik, 2008).

Such high loading levels will have a negative effect on the mechanical properties of the composites which can be used as flame retardants.

1.2.6.2 Magnesium Hydroxide

Usage of Magnesium hydroxide is less common than ATH. It decomposes through an endothermic reaction and evolved water as shown in Reaction1.15.

$$Mg(OH)_2 \longrightarrow MgO + H_2O \quad (1.15)$$

Thermal decomposition enthalpy value is between 1244 and 1450 Jg^{-1} (Lewin & Weil, 2001; Horn, 2000; Rothon, 2003; Rothon & Hornsby, 1996).

Furthermore, there are several theories related with the the exact mechanism of decomposition (Rothon, 2003; Green, 1983; Brett & MacKenzie & Sharp, 1970).

On the other hand, the magnesium oxide decomposition product maintains the original hexagonal structure of the magnesium hydroxide crystals that affects the fire retardant properties of formed magnesium oxide crystals (Hornsby & Watson, 1990).

Magnesium hydroxide can be used with some polymers, such as polyamides (Rothon & Hornsby, 1996). The loading levels of magnesium hydroxide is about more than 50 percent by weight for the requirements of good fire retardant properties.

Hornsby (Hornsby & Watson; 1986; 1989; 1990) has proposed the five possible fire retardant mechanism of magnesium hydroxide as follows;

1. Endothermic decomposition caused to decrease the thermal decomposition of temperature of the polymer in the composite
2. Release of water vapor diluting the vapor phase
3. The heat capacity of both the magnesium hydroxide and the decomposition product, magnesium oxide, further reduces the thermal energy available to degrade the polymer
4. The decomposition products promote char formation and therefore insulate the substrate from the heat source
5. The high loading level of magnesium hydroxide acts as a solid phase diluent

The high surface area of magnesium oxide acts as a smoke suppressant by absorbing carbonaceous decomposition products and may also catalyze their oxidation (Hornsby & Watson, 1990).

Magnesium hydroxide and aluminum hydroxide can also be used as smoke suppressants (Hornsby & Watson, 1989).

It has been ruled out a redox reaction between carbon and the metal oxide. As a result, smoke reduction occurs since they are refractory materials and cannot be reduced by carbon under combustion conditions (Hornsby & Watson, 1989).

It has been also suggested that the smoke suppression mechanism is the deposition of carbon on the surface of the magnesium oxide formed during combustion. The carbon products subsequently volatilize on exposure to oxygen due to the dissociation of oxygen on the oxide surface at temperatures of 400℃ - 500℃. The oxygen radicals then react with carbon, forming oxides (Hornsby & Watson, 1989).

In some reports, magnesium hydroxide, talc, and zinc borate mixtures can give synergistic effects. This is due to the formation of a mass transfer barrier on the surface of the decomposing polymer which protects the related polymer (Kim, 2003; Durin-France, Ferry, Cuesta & Crespy, 2000).

1.2.6.3 Huntite and Hydromagnesite

These minerals are alternatives of aluminum hydroxide and magnesium hydroxide as fire retardants. Huntite which is one of the most important flame retardants (Kangal & Güney, 2006), was discovered by Honors Professor Walter Frederick Hunt (1982-1975) in University of Michigan, Ann Arbor, Michigan, USA, and chemist with the U.S. Geological Survey. Huntite formations include different types of minerals such as Hydromagnesite, Magnesite, clay minerals, Aragonite and Dolomite (Kangal, & Güney, 2005).

The potential fire retardant minerals were given in Table 1.1. In this table, Hydromagnesite was present. Natural Hydromagnesite has been discovered in mixed deposits with Huntite that is why the mixtures have generated interesting fire retardant properties.

Hydromagnesite and Huntite mixtures have been commercially used as fire retardants since the late 1980's. Georgiades (Georgiades, Larsson, & Pust, 1996) reported the reserves of deposits in Greece. This deposit is still consumed. On the other hand, the world's largest known reserves of Huntite, Hydromagnesite and their mixtures are in Turkey, operated commercially by Minelco.

The deposit normally consists of Huntite and Hydromagnesite with varying ratios in between 40-30% Huntite and 60-70% Hydromagnesite. Aragonite, Calcite and Dolomite minerals are also present as impurities. The mineralogical composition is as follows: Huntite (46%), Hydromagnesite (46%), Magnesite (4%), Aragonite (3%) and Calcite (1%). A typical chemical analysis of the ore is MgO (38.0%), CaO (9.5%), H_2O (9.1%), CO_2 (43.4%) and LOI (52.5%). Huntite and Hydromagnesite consist of two distinct carbonates. Densities, chemical formulas and stability temperatures of Huntite and Hydromagnesite were given in Table 1.2, respectively (Kirschbaum, 2001).

Table 1.2 Formulas and properties of Huntite & Hydromagnesite (Kirschbaum, 2001).

Name	Formula	Density	Temp. Stability
Huntite	$Mg_3Ca(CO_3)_4$	2.70 g/cm^3	>400ºC
Hydromagnesite	$Mg_4(OH)_2(CO_3)_3.3H_2O$	2.24 g/cm^3	240-250ºC

Huntite particles have a fine highly platy structure as shown in SEM image in Figure 1.5 given by Hollingbery and Hull (Hollingbery, & Hull, 2010). Samples were gold coated and examined using a Carl Zeiss (Leo) 1530VP FEGSEM. Many of the individual particles have a diameter of 1 micron or less and thicknesses in the nanometer range.

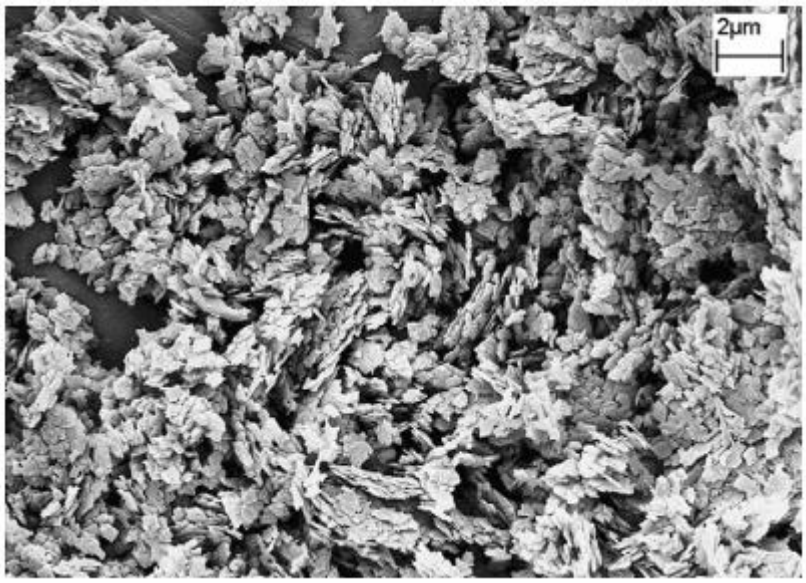


Figure 1.5 SEM Images of Huntite particles (Hollingbery, & Hull, 2010)

Thermogravimetric analysis (TGA) of Hydromagnesite and Huntite and their mixtures were studied and presented by Hollingbery and Hull. They are commercially produced by Minelco under the UltraCarb trade name (Hollingbery, & Hull, 2010).

In these analyses, Decomposition of Hydromagnesite begins to occur at 220 ℃ and progresses through two major mass losses. These mass losses have been reported (Beck, 1950; Padeste, Oswald, & Reller, 1991; Sawada, Uematsu, Mizutani, & Kato, 1978a; 1978b; Sawada et. al., 1979a; 1979b; 1979c; Todor, 1976). The reactions are as follows; firstly the loss of water of crystallization as in reaction (1.16),

$$Mg_5(CO_3)_4(OH)_2.4H_2O \longrightarrow Mg_5(CO_3)_4(OH)_2 + 4H_2O \quad (1.16)$$

Followed by decomposition of the hydroxide ion:

$$Mg_5(CO_3)_4(OH)_2 \longrightarrow Mg_4(CO_3)_4 + MgO + H_2O \quad (1.17)$$

Finally followed by decomposition of the carbonate ion:

$$Mg_4(CO_3)_4 \longrightarrow MgO + 4CO_2 \quad (1.18)$$

Huntite begins to endothermically decompose (Faust, 1953; Ozao, & Otsuka, 1985; Kangal, & Güney, 2006) at about 450 ℃ and progresses through two major mass losses in Figure 1.6. Initially it decomposes to magnesium oxide, calcium carbonate and carbon dioxide:

$$Mg_3Ca(CO_3)_4 \longrightarrow 3MgO + CaCO_3 + 3CO_2 \tag{1.19}$$

This is followed by the decomposition of calcium carbonate to calcium oxide and carbon dioxide:

$$CaCO_3 \longrightarrow CaO + CO_2 \tag{1.20}$$

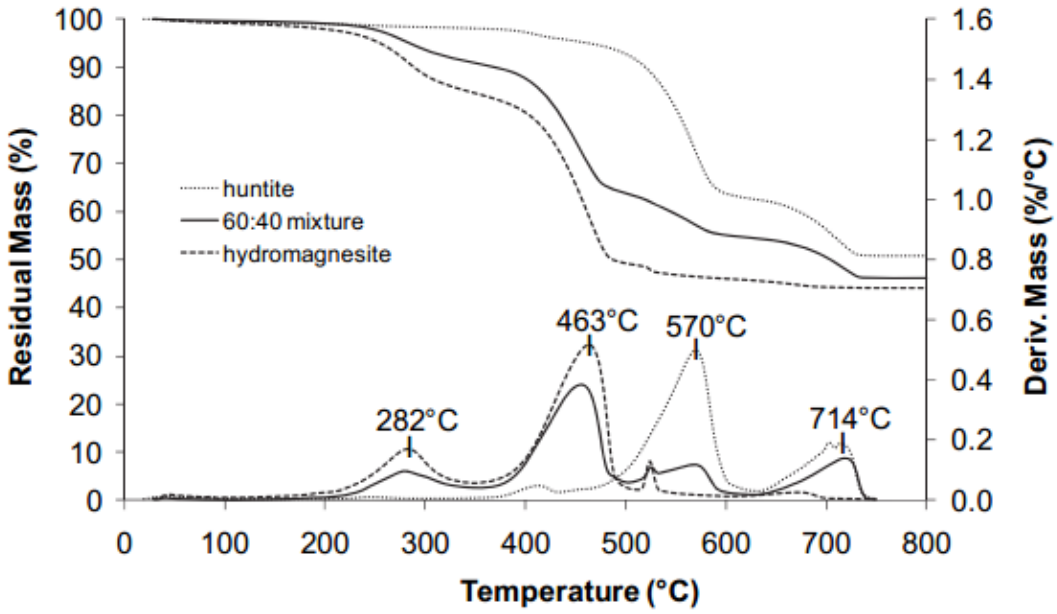


Figure 1.6 TGA profile of natural Hydromagnesite, Huntite and a 60:40 mixture of Hydromagnesite and Huntite (Hollingbery, & Hull, 2010)

It has been known that metal hydroxides act as effective fire retardant additives in polymer composites. The decomposition temperature of the polymer must be close to the endothermic decomposition temperature of the metal hydroxide (Hornsby, & Watson, 1989; Hornsby, & Watson, 1986; Hornsby, & Watson, 1990). The rate of polymer decomposition is therefore slowed because of the heat absorbed by the decomposing metal hydroxide and the released water dilutes the flammable polymer

decomposition products. The metal oxide residue also acts as a thermal barrier to further decomposition of the underlying polymer.

A mixture of Hydromagnesite and Huntite meets all of the above requirements and compared to the commonly used metal hydroxides may well provide some further benefits. The decomposition temperature of Huntite is high as compared with ATH and MH for the usage of fire retardancy in polymers. However, it may be useful in high temperature polymers such as polyetheretherketone (PEEK). Studies of the decomposition mechanisms of this polymer show that it does not begin to decompose until 575 ℃ (Patel et al., 2010). PEEK's melting point of 343 ℃ makes both aluminum hydroxide and magnesium hydroxide unsuitable. Huntite's initial decomposition temperature of about 400 ℃ and endothermic release of carbon dioxide up to 750 ℃ makes it an interesting possible additive for this polymer. Of course, only pure Huntite would be suitable; any Hydromagnesite present would decompose during melt processing.

In mixtures with Hydromagnesite, Huntite's platy morphology may provide a barrier to the transport of combustible decomposition products to the flame. It may also enhance mechanical reinforcement of carbonaceous or inorganic char. Once formed into a char layer Huntite will also provide additional protection to the underlying polymer through further endothermic decomposition in response to high external heat fluxes. These functions will not be provided by magnesium hydroxide or aluminum hydroxide due to their complete decomposition at lower temperatures (Hollingbery, & Hull, 2010).

The advantages of this mineral are noncorrosive to process in the extruders, low smoke formation, no acid gas emission, halogen free, environmentally safe, recyclable, none corrosive, no limitation in colouring and low combustion. Huntite and Hydromagnesite offer also effective cost and performance relationship in flame retardant applications (Weber, 1999).

The flame retardancy of Huntite/hydromagnesite was investigated for electrical applications (Yılmaz & Çelik, 2007). The minerals were characterized well and flame retardancy tests were done accordance with the UL94 standards.

1.2.7 Synergism

Synergism is often used in the optimization of flame retardant formulations but it is misinterpreted. Synergism means enhanced performance of the mixture of two or more components compared to the simple additive performance of the components at the same concentration (Weil, 1975).

Some examples and mechanisms of synergism are given and defined well (Alexander & Charles, 2007).

Halogen-free systems have great attention to enhance the fire retardant performance of aluminum hydroxide (ATH) and magnesium hydroxide (MH). It has been observed that combination of ATH and MH can be synergistic (Weil, 1999).

This effect is probably related with the elimination of water during the decomposition. Combinations of MH and zinc borate in the usage in poly(ethylene-co-vinyl acetate) were found to be synergistic. It was found that zinc borate catalyzes the dehydration of MH. In addition, zinc borate sinters properly the MgO particles (Weil et al. 2004).

1.2.8 Criteria for Selection of Flame Retardants

Criteria for the selection of flame retardants are usually based on:

- The efficiency of flame retardant in a particular polymer system
- The processing conditions of the polymer
- Compatibility and the ability to preserve valuable physical properties
- The cost-performance trade-off

Inorganic hydroxides are used at very high loading levels. Only certain polymers can tolerate such high loadings without a significant loss in mechanical properties. Furthermore, ATH due to relatively low thermal stability limits the usages of inorganic hydroxides. ATH is used in PVC, unsaturated polyesters, and latex back coatings of polyamide or polyester carpets (Alexander & Charles, 2007).

1.3 Nanocomposites

In recent years, polymer nanocomposites have expanded greatly and can be used in the field of fire retardancy. Indeed, clays and clay minerals can be combined with polymers in low amounts for the production of new composites with improved properties. Therefore, the study on polymer nanocomposites is not just about capturing the buzz from nanotechnology. In this area, structure-property relationships and interfacial phenomena are very important at the molecular and macromolecular scale.

There are many materials combined with clays have been investigated for many potential applications. Flammability applications for polymer clay nanocomposites were discovered a little later. Recently, new composite materials were prepared and provided into commercial use. Polymer nanocomposites for flammability applications are attractive because the formation of a nanocomposite not only improves the fire properties but can also improve other properties such as mechanical properties and bring the multifunctionality to the materials.

Multifunctionality is very important for polymer composites by having one material to do several works. For instance, a plastic case for an electronic device can have several requirements. It will require particular mechanical properties such as modulus, impact strength and thermal properties, flammability properties and electromagnetic properties as frequency shielding. For a commercial product, cost, density, color, and recyclability will need to be taken into account.

Polymer nanocomposites have shown great improvements over traditional composites in mechanical, thermal, gas barrier, conductivity, flammability, electromagnetic shielding, and other properties (Alexander & Charles, 2007).

1.4 Fire Tests and Standards

The flammability of polymers can be defined by their ignitability, flame spread rate and heat release properties. Depending on the targeted application of the polymeric material, one or more flammability criteria need to be measured (Laoutid etal. 2009).

1.4.1 Limited Oxygen Index (LOI)

LOI was first developed in 1966 by Fenimore and Martin (Fenimore & Martin, 1966). It is used to define the relative flammability of materials. The LOI standarts are in France (NFT 51-071), in the United States (ASTM D 2863) and an international standard (ISO 4589). The value of the LOI is defined as the minimal oxygen concentration, $[O_2]$ in the oxygen/nitrogen mixture $[O_2/N_2]$ that either maintains flame combustion of the material for 3 min or consumes a length of 5 cm of the sample, with the sample placed in a vertical position (the top of the test sample is inflamed with a burner). The LOI is expressed as:

$$\mathrm{LOI} = 100\,\frac{[O_2]}{[O_2]+[N_2]} \qquad 1.21$$

According to ISO 4589, the LOI is measured on ($80 \times 10 \times 4$ mm^3) specimens placed vertically at the center of a glass chimney (Figure 1.7). The mixture of gases flows upstream through this chimney and is homogenized by being passed through layers of glass beads. After a 30s purge of the column, the top of the specimen is ignited, like a candle.

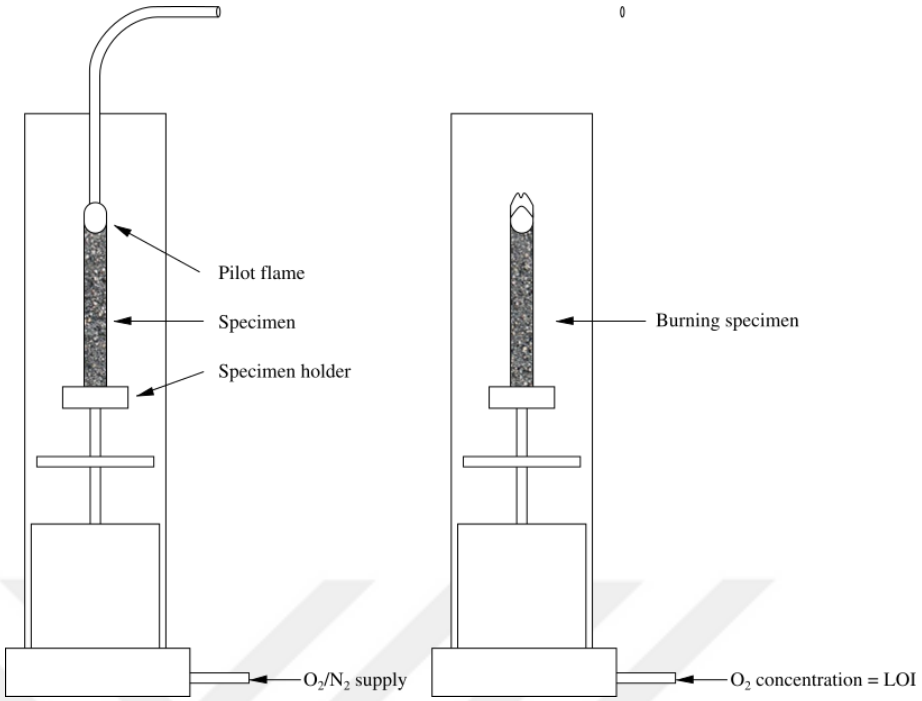


Figure 1.7 Experimental Set-up for LOI measurement (Charles & Alexander, 2009).

Materials with an LOI below 21% are classified as “combustible’’ whereas those above 21% are classified as ‘‘self-extinguishing’’. The higher the LOI is the better the flame retardant property.

Although this test is nowadays considered to be relatively unsophisticated due to the development and standardization of more elaborate methods, it remains one of the most important screening and quality control methods used in the plastics industry (Laoutid et al. 2009).

Table 1.3 lists flash ignition and self-ignition temperatures for various polymers, together with their LOI values.

Table 1.3 LOI, flash- and self-ignition temperatures of selected polymers (Laoutid et al., 2009).

Polymer	Flash-ignition temperature (ºC)	Self-ignition temperature (ºC)	LOI (%)
Polyethylene	340	350	18
Polypropylene	320	350	18
Polystyrene	350	490	18
Poly(vinylchloride)	390	450	42
Poly(tetrafluoroethylene)	560	580	95
Poly(methylmethacrylate)	300	430	18
Poly(acrylonitrile)	480	560	27
Polyamide6	420	450	25
Polymaide66	490	530	24

1.4.2 UL 94 Vertical Test

UL94 tests has been developed by the Underwriters' Laboratories as tests of the flammability of plastic materials. It covers vertical and horizontal flammability tests. UL94 V is used commonly for measuring the ignitability and flame-spread of vertical bulk materials exposed to a sma ll flame. This test is carried out according to the IEC 60695-11-10 standarts for small flames (50W). It is a simple test of vertical combustion that classifies the composite materials as V0, V1 or V2 rates. The corresponding experimental device is schematically shown in Figure 1.8.

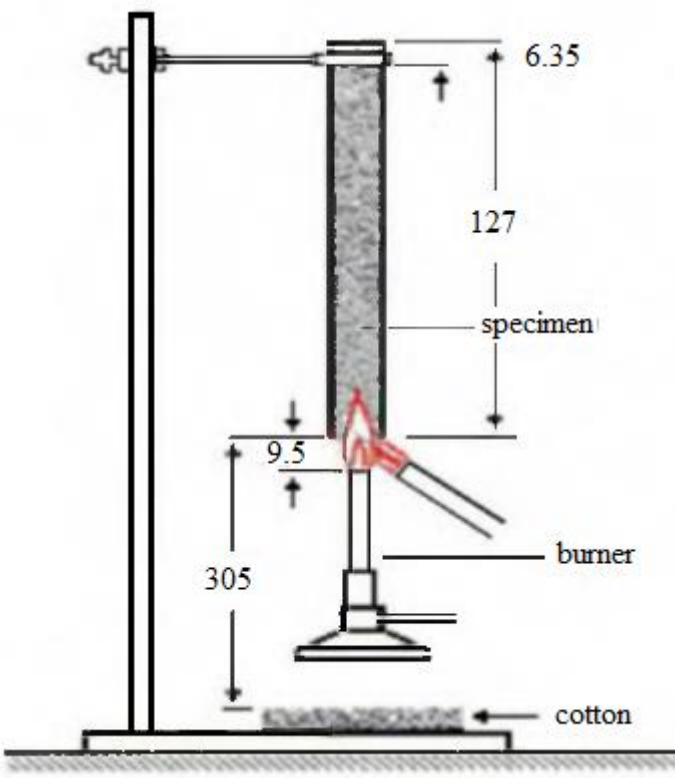


Figure 1.8 Experimental Setup for UL94 Vertical Test (Laoutid et al., 2009; Yıdırım, 2013)

The burner is controlled to produce a blue flame with a 20 mm high central cone and a power of 50 W. The flame is applied to the bottom of the specimen and the top of the burner has to be located at 10 mm from the bottom edge of the specimen. The flame is applied for 10 s and removed. The after flame time t1 (the time required for the flame to extinguish) is noted. After extinction, the flame is applied for another 10 s. The after flame time t2 is noted, together with the after glow time t3 (the time required for the fire glow to disappear).

During the flame application, the distance between burner and specimen must remain constant. If drops fall, the burner must be tilted through a maximum angle of 45º or slightly isolated from the specimen flame. In the test five specimens must be tested (Laoutid et al. 2009).

The classification is V0, V1 or V2 as in Table 1.4.

Table 1.4 UL 94 flammability test classification of the materials (Laoutid et al. 2009).

Fire Classification	Description
V0	t_1 and t_2 less than10 s for each specimen,
	$t_1 + t_2$ less than 50 s for the five specimens,
	$t_2 + t_3$ less than 30 s for each specimen,
	No after flame or after glow up to the holding clamp, No burning drops.
V1	t_1 and t_2 less than 30 s for each specimen,
	$t_1 + t_2$ less than 250 s for the five specimens,
	$t_2 + t_3$ less than 60 s for each specimen,
	No after flame or after glow up to the holding clamp, No burning drops.
V2	t_1 and t_2 lessthan 30 sfor each specimen,
	$t_1 + t_2$ less than 250 sfor the five specimens,
	$t_2 + t_3$ less than 60 sfor each specimen,
	No after flame or after glow up to the holding clamp, Burning drops allowed.

The procedure was also outlined in details (Yıldırım, 2013).

1.5 Powder Coating

There are two principal technologies in the coatings industry. First one is well known liquid coating technology or wet technology. Second one is powder coating technology or dry techniques applied on industrial scale in recent years.

Main difference between a conventional liquid paint and a powder coating is that the powder coating does not require a solvent to keep the binder and filler parts in a liquid suspension form. Solvents contribute to air pollution and in some cases depletion. Furthermore, liquid paint contains much more volatile organic compounds and hazardous air pollutants, which both vaporize and enter the atmosphere and thus have a negative impact on the environment Moreover, solvent-based liquid paints often

result in significant waste as it is hard to recycle. In contrast, when using powder coatings the over-sprayed powder that does not adhere to the part can easily be retrieved and reused. It is practice that about 98-99% of the material is reused when powder coatings are chosen, whereas most of the conventional liquid paint is solvent and evaporates during application. This makes powder coating the ecological choice. Also with powder coating it is possible to reach higher film thickness, which gives higher coating quality. Powder coating application doesn't need any primer and powder doesn't need any pre application elaboration.

Because powder coatings are cured in an oven the drying time is shortened radically compared with solvent-based coatings. After less than 10-15 minutes in the oven the painted product is ready and therefore can be sent to the next step in the assembly (if so needed). Powder coatings can be applied much thicker than conventional liquid coatings without running or sagging.

Furthermore, a wide range of specialty effects can easily be accomplished with powder coatings. Some of these are for instance gauffered, textured, hammer-toned and metallic coatings. Because of the advanced methods with which powder coatings are applied, all types of powder coatings provide a durable, uniform and attractive finish (Akzo Nobel, 1999).

Powder coating is rapidly becoming the new standard for paint applications instead of liquid paint. Some of the reasons that powder coating is more efficient are a higher quality finish, no drying time and over-spray recovery. It shows significant durability and resistance to abrasion, corrosion, scratching, and chemicals when compared to liquid coatings (Mazumder & Wankum, 1997). It stays bright with less fading and color selection is virtually unlimited with high and low gloss, metallic and clear finishes (Kleber & Lang, 1997). Texture selections range from smooth surfaces to wrinkled and rough textures are available for hiding surface imperfections. Thick coatings can be achieved quickly and efficiently (Dastoori & Makin, 2001).

Compared with the 4,000 years that paints have existed, powder coatings have been around for no longer than the blink of an eye. Yet, it is already obvious that they are

revolutionizing the paint manufacturing and processing industries. In every respect, from paint processing and properties right through to economic considerations, ecology and paint consumption are very important (Mirabedini &Thompson, 2003). Powder coatings are currently the fastest growing section of industrial paints because of their favorable environmental attributes and performance advantages (Fuentes, Almandoz & Pierrugues, 2010).

1.5.1 Types of Powder Coating

There are two main categories of powder coating: thermosets and thermoplastics. The thermosetting variety incorporates a cross-linker into the formulation. When the powder is baked, it reacts with other chemical groups in the powder to polymerize, improving the performance properties. The thermoplastic variety does not undergo any additional actions during the baking process, but rather flows to form the final coating.

The most common polymers used are polyester, polyurethane, polyester-epoxy (known as hybrid), straight epoxy (fusion bonded epoxy) and acrylics (Powder coating, https://en.wikipedia.org/wiki/Powder_coating, 2017).

***Epoxy powders*:** can be formulated to give high gloss and smooth coatings with excellent adhesion, flexibility and hardness as well as solvent and chemical resistance. The main deficiencies are their poor tolerance to heat and light as well as their pronounced tendency to yellow at elevated temperatures and exposure to diffused day light.

***Acrylic powders*:** are widely used in surface coatings. They have good gloss and color retention on exterior exposure as well as heat and alkali resistance.

***Polyester powders*:** general performance can be categorised between epoxy and acrylic powders. They have excellent durability and a high resistance to yellowing under ultraviolet light. Most coatings used on buildings today.

***Polyurethane powders*:** provide good physical and chemical properties as well as high exterior durability.

***Epoxy polyester hybrid powders*:** are epoxy powders by containing a high percentage of special polyester resins. These hybrids have properties similar to those of epoxy powders. Their advantage is that they have improved resistance to overtake yellowing and weather stability. Hybrid powders are now regarded as the main backbone of the powder coatings industry. They are mostly used for consumer goods, metal furniture, ceiling panels in the building industry, shower cabins, automotive components, agricultural equipment and machinery and shelves (Akzo Nobel, 1999).

In this study, we have used epoxy polyester hybrid powders for resin.

1.5.2 Powder Coating Formulations

As with any coating, formulation variables are critical to the processing and performance characteristics. The powder coating formulation is much like a liquid coating formulation except that most of the components are in solid, melt process able form. The main raw material components used in powder coatings are described below.

Resins are the key component. The ranges of resin used are increasing steadily in an attempt to meet the more demanding needs of new market sectors. For example silicone which shows high heat resistance capability.

Pigments are generally solid particulate materials such as titanium dioxide, carbon black or inorganic metal oxide pigments.

Fillers are used to reduce the cost of the coating formulation and to improve specific properties such as flow, surface texture, lubricity, etc. Common fillers are barytes, calcite, mica, talc, whiting, etc.

Matting agents are used to reduce the gloss of the cured film.

Waxes are added to the formulation to provide slip, hardness, scratch and mar and to act as free flow powders and anti-bridging agents in processing.

Texturing agents are used to control or enhance the gloss level of cured films.

Flow agents enhance film properties and minimize surface defects by improving the flow of the molten coating. Examples of flow agents include polyacrylates, silicones, surfactants, and fluorinated alkyl esters (Mirabedini &Thompson, 2003).

1.5.2.1 Fillers

In the experiment, Barium Sulphate (Filler26), Huntite and Magnesium carbonate hydroxy hydrate (MCHH) were used as filling metarial.

1.5.2.1.1 Barium Sulphate. Baryte is a sulfate of barium with chemical formula of $BaSO_4$. It is generally white or colorless, chemically inert, insoluble in water, with high density, and the main source of barium. Although baryte contains a "heavy" metal (Barium), it is not considered to be a toxic chemical reagent by most governments because of its extreme insolubility (Hanor, 2000). Commonly, baryte is used for the production of barium hydroxide for sugar refining and as a white pigment for textiles, paper, and paint (Dana & Ford, 1929). It is also suitable for other purposes due to its high specific gravity (4.5), opaqueness to X-rays, inertness, and whiteness (Shen et al., 2007). Recently, more attention has been paid on the massive production of $BaSO_4$ nanoparticles for its multiple applications in the oil industry, electronics, TV screen, glass, car filters, paint industry, and ceramics as well as in medical applications (Ramaswamy et al., 2011). Recently, barite has been incorporated into polymers to form electrical-insulating barite/epoxy composites with X-ray attenuation properties (Unsworth et al., 1993). $BaSO_4$ is used in paints and coatings for stabilization of pigments against flocculation and show high transparency (Vogelsberger et al., 2011).

1.5.3 Producing Industrial Powder Coatings

According to the report (Akzo Nobel, 1999), production of industrial powder coatings based on four steps. These are weighing, premixing and size reduction of raw materials, extrusion of pre-mix, cooling and crushing of the extrudate into chips, micronising the chips into the final powder and post mixing, packaging and storage.

Weighing, premixing and size reduction of raw materials - Raw materials typically consist of resin, curing agents, pigments, extenders and additives. Each of them must pass the quality controls. Each component is then weighed accurately. According to the formulation, all components are placed in a mixing container and thoroughly mixed by cutting blades for a period of time. The raw materials can also be reduced in size to improve the melt mixing later in the process (Akzo Nobel, 1999).

Extrusion of the premix - The mixture is fed into the extruder. The extruder barrel is maintained at a predetermined temperature in between 70-120 ºC, depending the product type. The barrel temperature is set so that the resin is only just liquefied and its contents are mixed using the screw in the barrel. Consequently, it produces a homogeneous composite (Akzo Nobel, 1999).

Micronising of the chip into the final powder – The chips are ground to the required particle size in a grinding mill and fed onto an enclosed grinding wheel with stainless steel pins for the production of powder (Akzo Nobel, 1999).

1.5.4 The Powder Coating Application

The powder coating application involves three basic steps:

1. **Pre-treatment**: Parts that are to be powder coated needs to be properly pre-treated to reach excellent result. Before the parts are to be powder coated they need to be washed properly.

2. **The powder application**: When applying the powder coating to metal objects a gun is used to spray the powder on the part desired to be painted. The gun imparts a negative electric charge on the powder, which is then sprayed towards the object which in turn sticks on it. In the next step the object is heated, and the powder melts and then cures into a uniform film.

3. **Curing**: When the powder has been sprayed and attached on the object it is exposed to cure temperature, so that it can begin to melt, flow out and cure. Thus, it chemically reacts to form a higher molecular weight polymer, in a network-like structure. The curing can be completed in convection cure ovens or infrared cure ovens. The cure process requires a certain degree of temperature for a certain length of time to establish the full film properties that the material was designed for. Normally the powders cure at 200 ℃ in 10 minutes.

1.6 The Aim of the Thesis

In recent years, the demands for less flammable polymers in the industry have changed from ignition suppression to lower smoke and toxicity, to "halogen-free" polymer composites. In the near future, sustainable fire retarded materials will be greatly required.

Metal hydroxides are effective flame retardants and cover about 40% by weight of the total flame retardant market. Their fire retardancy is due to the endothermic decomposition with the release of water. The two most commonly used mineral flame retardants are aluminum trihydroxide, $Al(OH)_3$, (ATH) and magnesium hydroxide, $Mg(OH)_2$, (MH). They are known as the most effective halogen free fire retardants which start releasing water vapor at approximately 200 and 300 ℃, respectively. As a result of this mechanism, they do not introduce any corrosive or potentially toxic substances and also give low smoke levels. The residues mainly composed by Al_2O_3 and MgO, respectively. The decomposition must occur above the polymer processing temperature and close to the polymer pyrolysis temperature. Their flame retardant effects are quite similar, but aluminum hydroxide is less expensive to produce in a useful form and thus has most of the market. Magnesium hydroxide is more stable and

mainly used where the processing temperature would be too high for aluminum hydroxide. Several studies reported on the use of a number of other hydroxides and hydroxy carbonates, such as Boehmite, Hydrotalcite, Hydromagnesite, Clays, Clay Minerals and Hydromagnesite/Huntite hybrid compound, which could be used as alternative to halogen fire retardant additives.

Magnesium hydroxide and magnesium carbonates such as Huntite and Hydromagnesite are endothermic flame retardants and smoke suppressants utilized in applications where higher processing temperatures are necessary, and they are sufficiently stable to be incorporated into thermoplastics without decomposition. Huntite is used as flame retardant additive in various polymers like ethylene vinyl acetate (EVA), polypropylene (PP), polyethylene (PE), ethylene propylene copolymer, vinyl ester resin and poly vinylchloride (PVC).

The aim of this Thesis is to investigate and evaluate the use of minerals such as various metal hydroxides and metal carbonates based hydrated Huntite, Hydromagnesite/Huntite and Basic Magnesium Carbonate as flame retardant materials for polyester based polymers and resins as a basis for producing flame retardant electrostatic powder paint coatings. The products will then be characterized by TG/DTG, DTA, DSC, XRD, FTIR and SEM analysis. Their fire retardancy will also be determined by LOI and UL 94 tests. Schematic presentation of the aim of the thesis is given in Figure 1.9.

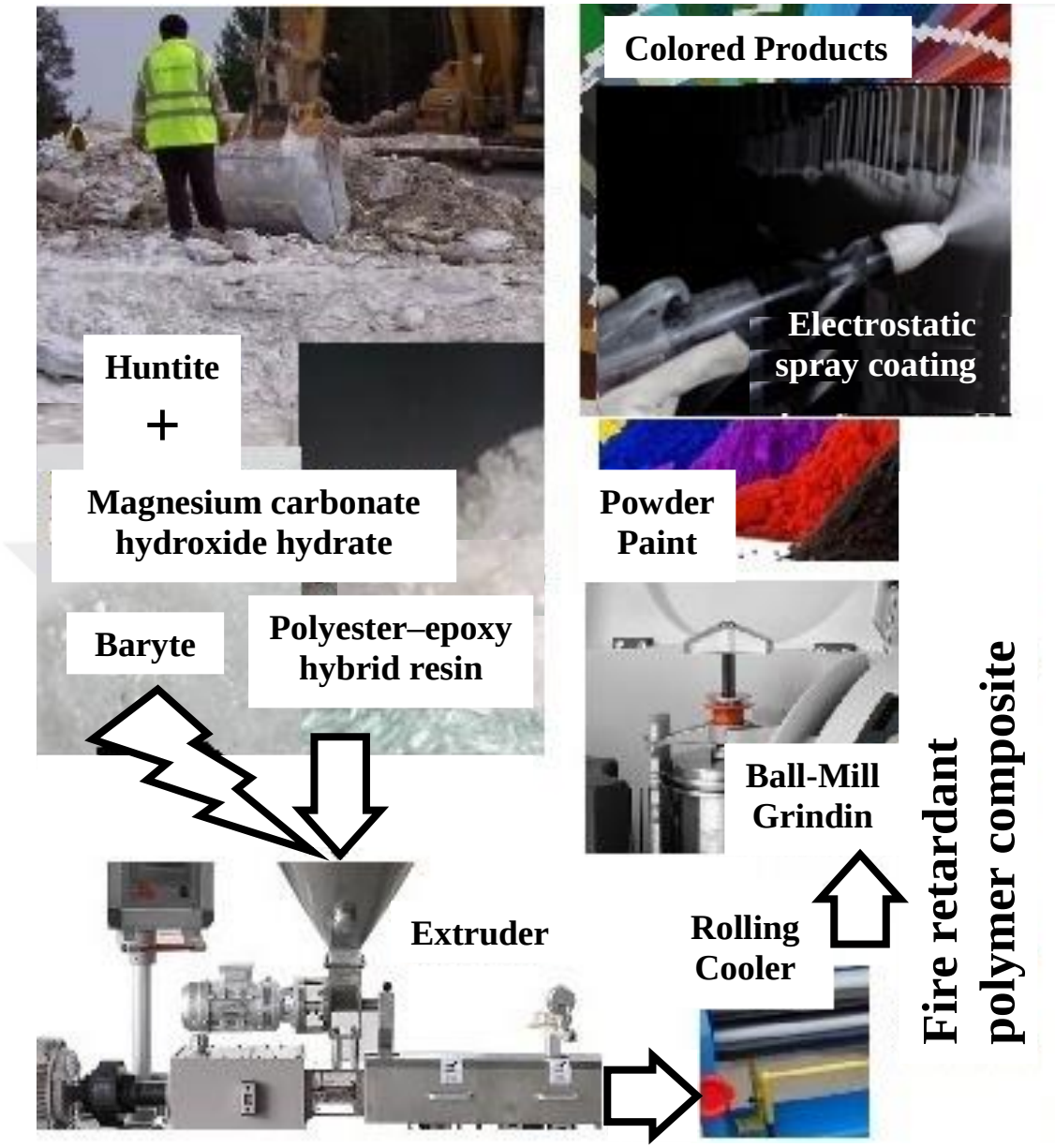


Figure 1.9 Schematic presentation of the aim of the Thesis

CHAPTER TWO
MATERIALS AND METHODS

2.1 Materials

Polyester resin (PE 6400) and epoxy resin (Epoxy GS 7351) were used as main matrix. Filler26 ($BaSO_4$), Kat012, Kat003 and P28 obtained from EKO Boya, Akhisar/Manisa-Turkey were used as filling material, flow agent, brightener and pigment, respectively. Huntite, $Mg_3Ca(CO_3)_4$, as flame retardant obtained from Acıpayam-Çameli Huntite mines in Denizli-Turkey. Magnesium carbonate hydroxide hydrate $C_4Mg_4O_{12}.H_2Mg_2O_2.xH_2O$, as flame retardant was purchased from Sigma-Aldrich (Cat. No. 227668, 99%).

2.1.1 Preparation of Polymer Composite Coatings

The formulation of the composites mainly included polyester, epoxy, Filler26 ($BaSO_4$) and flame retardants (Huntite and magnesium carbonate hydroxide hydrate). Composite formulations were arranged by adding different amounts (10%, 20%, and 30% etc.) of flame retardants to polyester-epoxy hybrid resin. The total amount of filling material (Filler26) was 43% in the product power coating (Plate 0). Flame retardants were used as a filling material. Therefore, Filler26 and flame retardants' total amount in the Plates were 43%. Polyester-epoxy hybrid resin (55 wt %), Filler26, PV88 (1 wt %), Kat003 (0.2 wt %), P28 black (1 wt %) and flame retardants were remixed. In these formulations, PV 88 used as flow modifier of paint during melt cure in the oven is a liquid acrylic polymer and has been converted into a free flowing powder by adsorption onto silica type filler. Kat003 is Benzoin and used for degasing of paint during curing process in the oven. P28 is a pigment and used as colourant. Then, the mixture was fed into the extruder. The extruder barrel is maintained at a temperature between 85-95ºC. In order to obtain the composites in powder, they were ground in a grinder. Uncured powder was then sprayed and charged electrostatically through spray guns onto the aluminum Plates which were cleaned by acetone before application. The Plates were cured at 200 ºC after the application for 10 min in a cure oven.

Sample code and composition of the composite samples as weight % are shown in Table 2.1. Preparations of polymer composite coatings were shown in Figure 2.1.



Figure 2.1 Preparations of polymer composite coatings

Table 2.1 Sample code and composition of the composite samples as weight %.

Sample	Polyester-Epoxy Hybrid resin	Filler26 ($BaSO_4$)	Flame retardants	
			Huntite	$C_4Mg_4O_{12}.H_2Mg_2O_2.xH_2O$
Plate 0	55	43	-	-
Plate 1	55	33	10	-
Plate 2	55	23	20	-
Plate 3	55	23	30	-
Plate 4	55	3	40	-
Plate 5	55	33	-	10
Plate 6	55	23	-	20
Plate 7	55	13	-	30
Plate 8	55	3	20	20
Plate 9	55	17.8	12.6	12.6

2.2 Fourier Transform Infrared Spectroscopy (FTIR) Analysis

FT-IR spectra of powder composites were recorded by FTIR Analyzer (Perkin Elmer Spectrum BX-II, USA) as pellets. 1 mgs of the samples was mixed with 100 mg of KBr. FTIR analyses were conducted after drying the pellets at 60 ^oC. The spectrum was recorded as 50 scans with a resolution of 2 cm^{-1} at the wavenumber range of 4000-400 cm^{-1}.

2.3 X-Ray Diffraction Analysis (XRD)

The X-ray diffraction patterns of the samples were recorded in Rigaku-Rint 2200/PC (Ultima 3) X-Ray diffractometer using Cu K_α radiation in the 2θ range of 10-90^o with a scanning rate of 0.4 degree/min.

2.4 Thermal Analysis

The thermal behaviors of the samples were investigated by TGA/DTG and DTA analysis. The analysis was conducted under nitrogen flow from room temperature to 900 ℃ at a heating rate of 10℃/min with a Perkin Elmer Diamond TG/DTA instrument. DTA analyses are performed in the temperature range of 25-600ºC at a heating rate of 10 ℃/min in nitrogen gas atmosphere by using Perkin Elmer DTA instrument.

DSC analysis was performed under nitrogen flow from 20℃ to 300℃ at a rate of 20℃/min with Perkin Elmer Diamond Differential Scanning Calorimetry (DSC) instrument in Central Research Laboratories of Middle East Technical University/Ankara-Turkey. The 3 and 5 mgs of samples were placed in an aluminum pan and sealed. Test specimens were heated from 20 ℃ to 300 ℃ at a heating rate of 20 ℃ min^{-1} in the first heating period and the temperature was held for two minutes at 300 ℃. After cooling from 300 ℃ to 20 ℃ at 20℃ min^{-1}, the samples were held for 2 min at 20 ℃. Then 2^{nd} heating period from 20 ℃ to 300 ℃ at 20℃ min^{-1} was conducted.

2.5 Scanning Electron Microscopy (SEM)

The surface morphologies of composites were studied at an accelerating voltage of 10 kV. SEM images were taken at different magnifications (in the range of 500–10,000X) by using Jeol JSM 60 model SEM apparatus equipped with energy dispersive X-Ray (EDX). The samples were used as powder form without coating in SEM experiments.

2.6 Flame Retardancy Tests (LOI and UL94 Tests)

LOI and UL94 tests are used for measuring flame-retardancy. LOI values were measured at room temperature by an Asian Oxygen Index Tester (India) according to ASTM D2863-1997 standard with specimen dimension of 110 × 6.5 × 2 mm^3. UL94 tests were performed on a self-asembly instrument as vertical and horizantal setups in

our laboratories according to UL94 test standard with specimen dimension of 110 × 3 × 2 mm^3. UL94 testing results were carried out for burning ratings V-0, V-1, or V-2. V-0 rating corresponds to the best flame retardancy of polymeric materials. ZLT-ZY2 Needle-Flame Tester Instrument was also used for flame retardancy tests.LOI Apparatus was presented in Figure 2.2. UL94 Vertical and Horizontal Test Setups were shown in Figure 2.3 and 2.4, respectively. ZLT-ZY2 Needle-Flame Tester Instrument was also shown in Figure 2.5.



Figure 2.2 LOI Apparatus

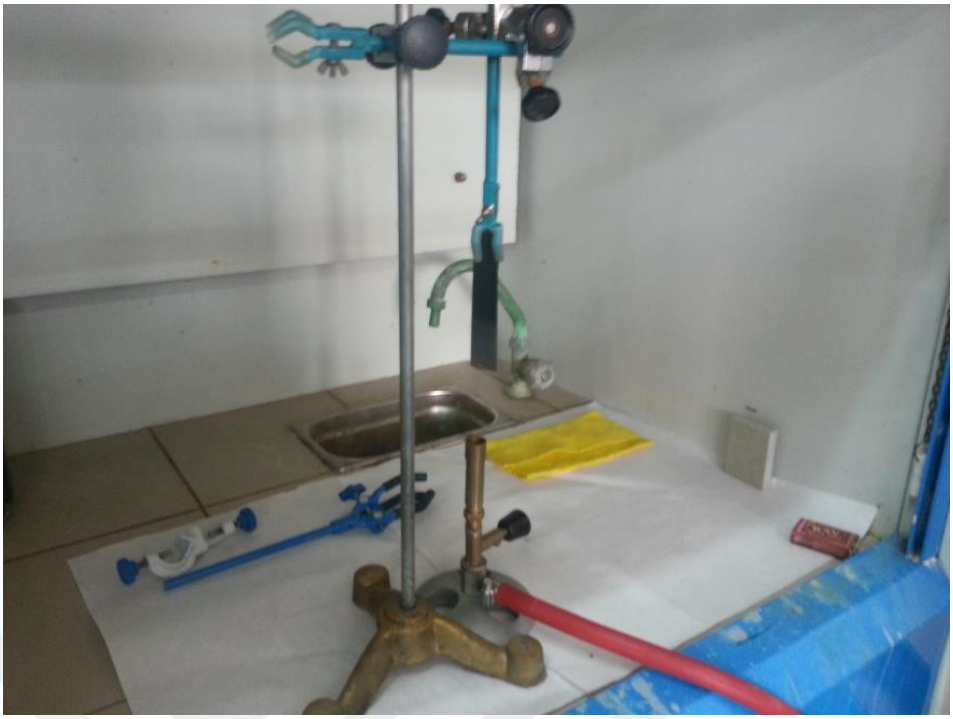


Figure 2.3 UL94 Vertical Test Setup



Figure 2.4 UL94 Horizontal Test Setup



Figure 2.5 ZLT-ZY2 Needle-Flame Tester

CHAPTER THREE
RESULTS AND DISCUSSION

3.1 X-Ray Diffraction (XRD) Analysis

The phase and crystallographic structure of the samples were identified from XRD patterns. XRD pattern of the Huntite was given in Figure 3.1. The powder XRD peaks are consistent with the data of the card 14-409 in the Crystallographica Search-Match (Version 2, 0, 3, 1) file of $Mg_3Ca(CO_3)_4$ with rhombohedral phase. Likely, XRD pattern of barium sulphate is shown in Figure 3.2. From this figure the characteristic peaks are identified as from (101), (111), (021), (121), (002) and (212) planes which shows the orthorhombic structured $BaSO_4$ (JCPDS card No.: 24-1035). XRD pattern of Magnesium carbonate hydroxide hydrate (MCHH) is shown in Figure 3.3. The XRD patterns of the samples were also examined. It can be seen that the XRD pattern of the $BaSO_4$ displays the following diffraction peaks (2θ/°): 20.58°, 22.88°, 24.96°, 25.98°, 26.96°, 28.86°, 31.62°, 32.94°, 42.74° and 43.04° which can be correlated to the (hkl) indices (020), (101), (111), (200), (021), (210), (121), (211), (002) and (140), of Barite (JCPDS No: 83-1718 and JCPDS No: 24-1035). All the samples have an intense peak at 2θ=42-43° which is a characteristic feature of $BaSO_4$composed mainly from Barite. The samples displayed the typical orthorhombic structure of $BaSO_4$. The diffraction peaks of (hkl) values (101), (111), (021), (121), (002) and (212) were the characteristics of orthorhombic $BaSO_4$ crystals. The patterns were basically in agreement with the reported values (Shen et. al., 2007; Ramaswamy et. al., 2011; Salah et. al., 2009). Impurities such as SiO_2 and $SrSO_4$ were also observed.

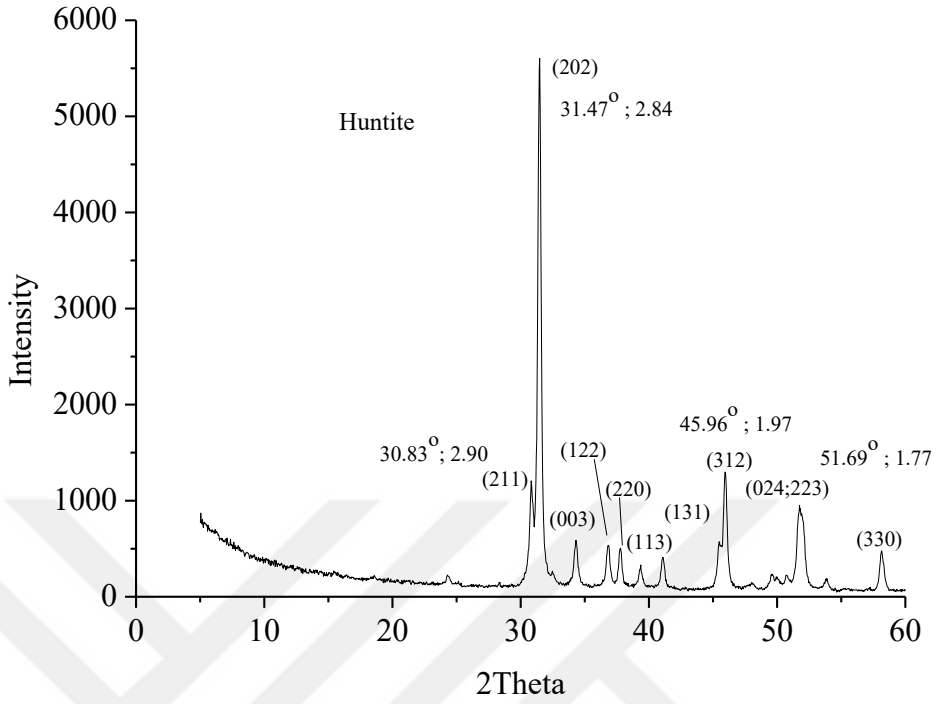


Figure 3.1 XRD patterns of Huntite

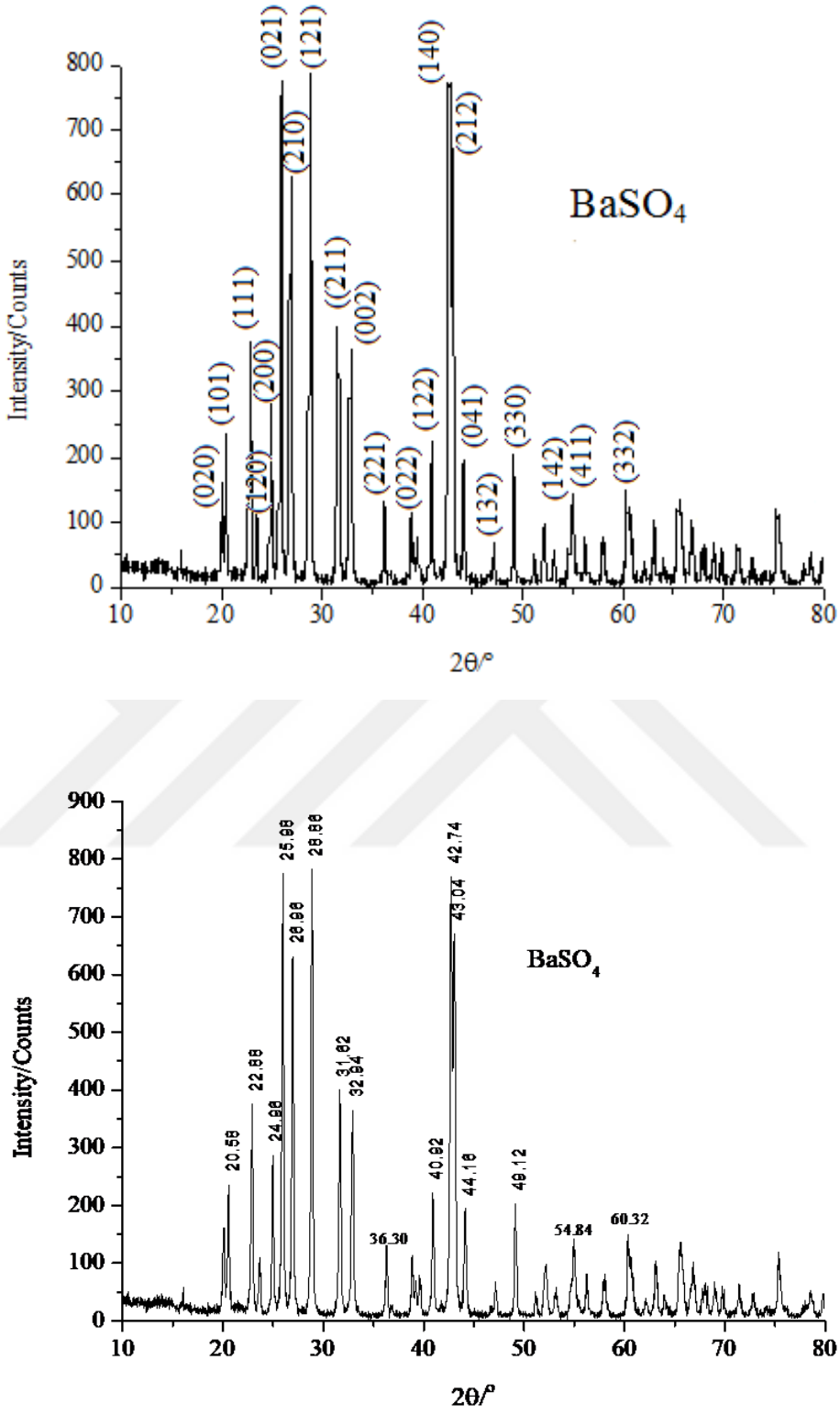


Figure 3.2 XRD patterns of Barium Sulfate

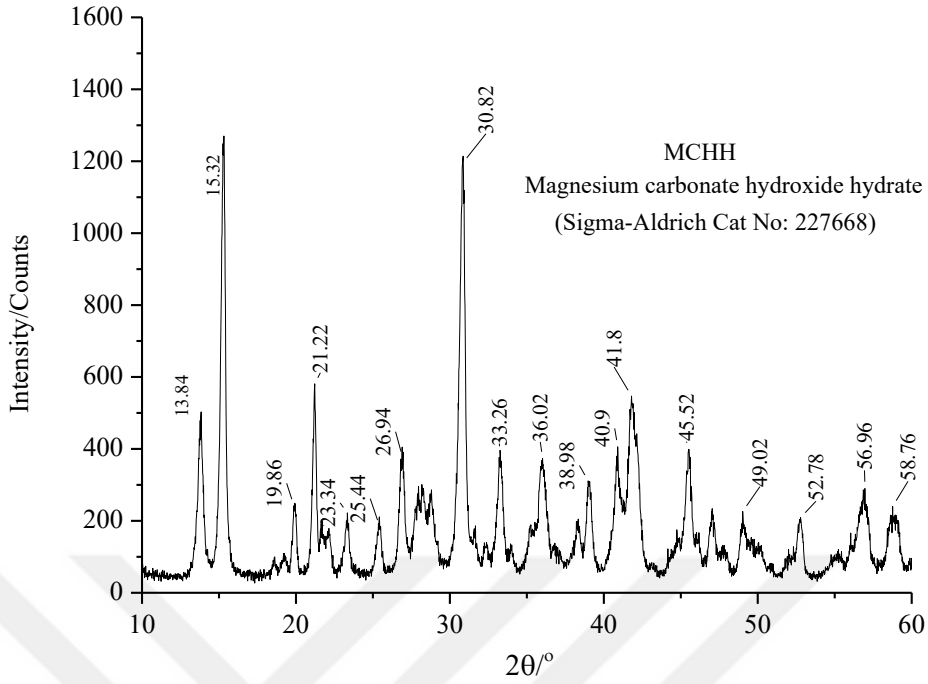


Figure 3.3 XRD patterns of MCHH

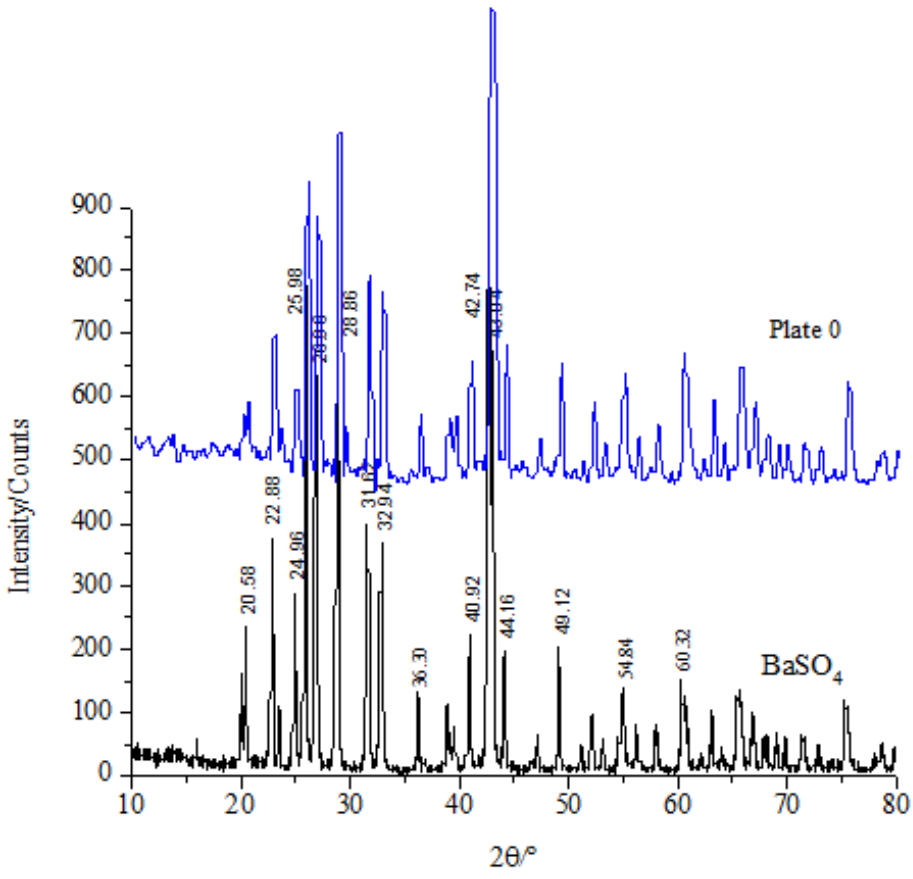


Figure 3.4 XRD Patterns of $BaSO_4$ and Plate 0

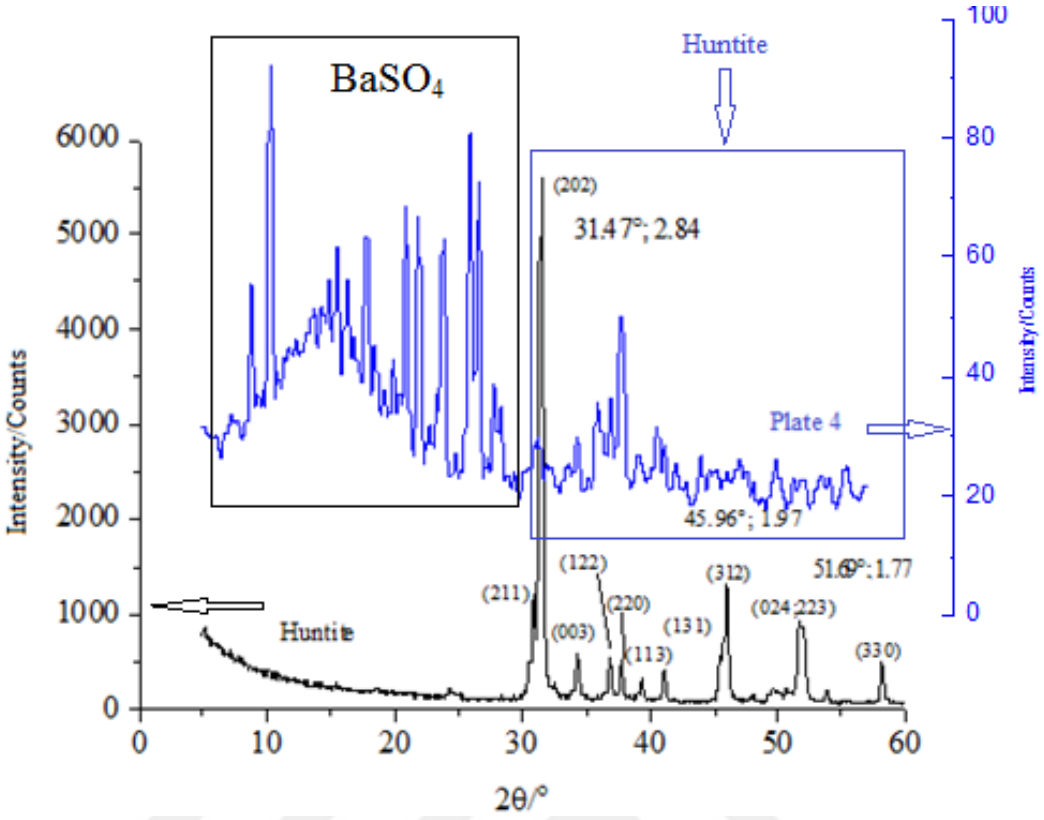


Figure 3.5 XRD Patterns of Huntite and Plate 4

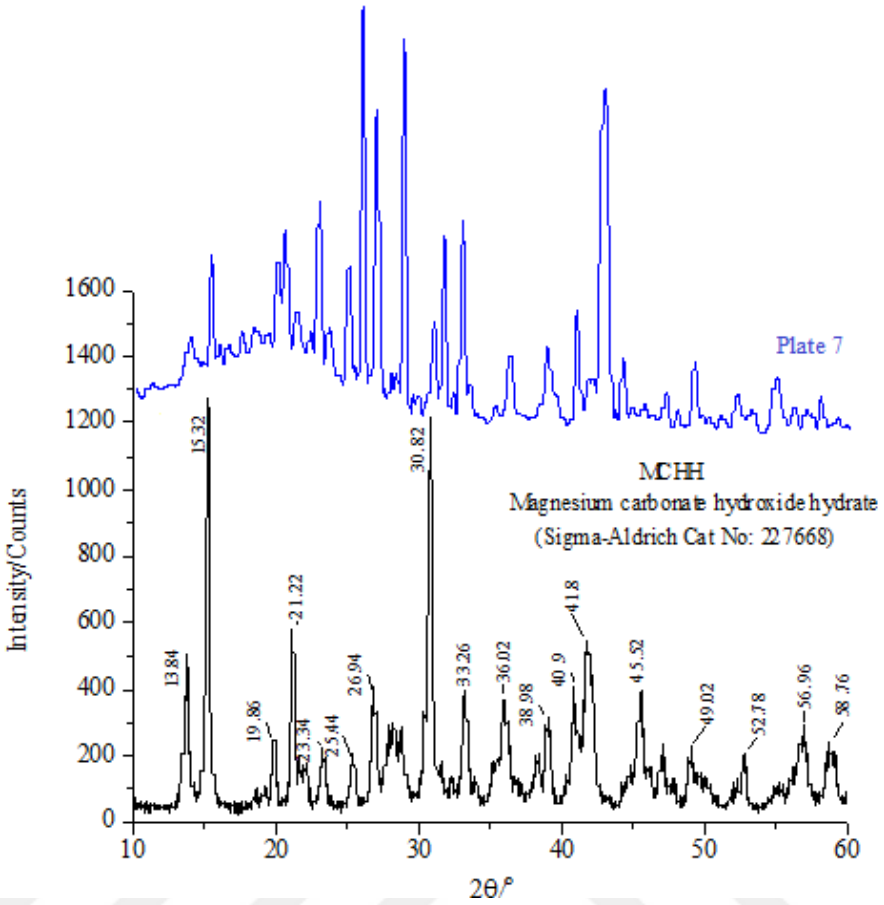


Figure 3.6 XRD Patterns of MCHH and Plate 7

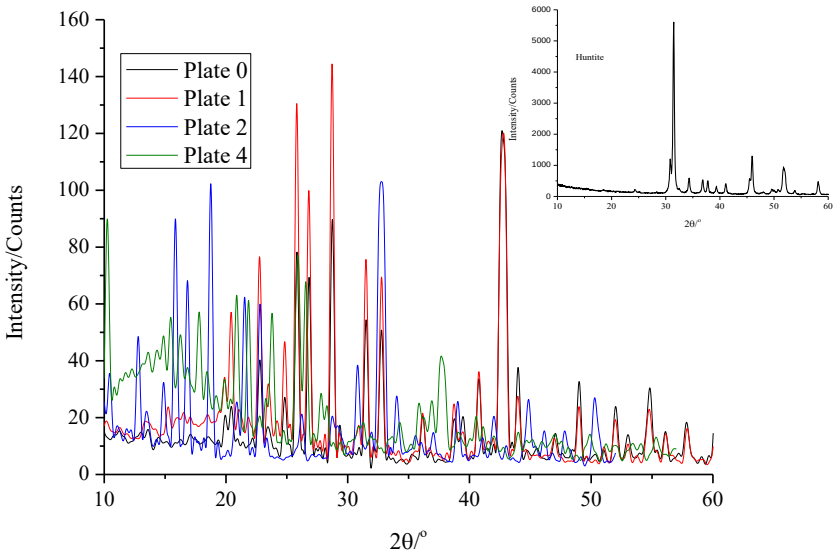


Figure 3.7 XRD Patterns of Huntite and Plate 0, 1, 2 and 4

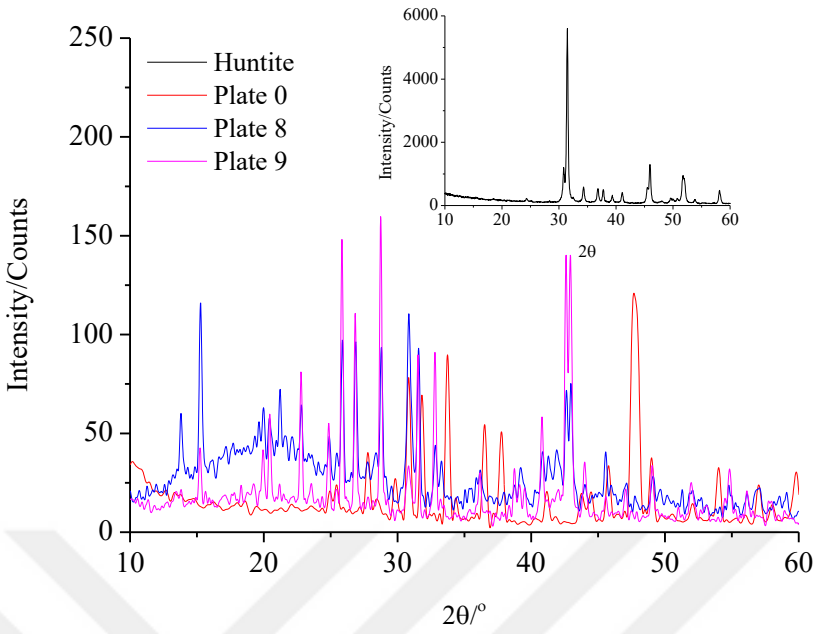


Figure 3.8 XRD Patterns of Huntite and Plate 0, 8 and 9

In the XRD patterns of the samples (see Figure 3.4 - Figure 3.8), it has been observed that the signal intensities of the peaks for the Plates were so weak (less than 200 counts) and complex as compared with the intensities of Huntite, $BaSO_4$ and MCHH. The peaks of the Plates were blunted due to the matrix effect of pure materials.

3.2 Scanning Electron Microscopy (SEM) Analysis

The surface morphology of Huntite, Synthetic basic magnesium carbonate [$(MgCO_3)_4 \cdot Mg(OH)_2 \cdot \times H_2O$], Filler26- Barium sulphate were studied by using SEM analysis. SEM results were presented in Figure 3.9 - Figure 3.11. Naturally occurring Huntite particles have a fine highly platy structure as shown in the electron micrographs (Figure 3.9). The basic magnesium carbonate particles have a fine highly platy structure and compact earthy structure as shown in the electron micrographs (Figure 3.10).The Filler26- Barium sulphate particles have spherical shell types of nanoparticles and granular structure as shown in the electron micrographs (Figure 3.11).The formation of the mesoporous structure is related both to nucleation and to the growth mechanism of the $BaSO_4$ particles (Nagaraja et al., 2007).

In order to determine the surface morphologies of the composites, SEM images at different magnifications were recorded and shown in Figure 3.12. It has been observed that the composite coatings are more rough and tough than pure dye. The presence of Huntite particles detached from the polyester matrix is obvious from the fracture surface (Figure 3.12 b-e). Figure 3.12 b-d shows the unhomogeneous dispersion of Huntite particles into composite. Based on morphological study (shown in Figure 3.12 b-e), it is found that Huntite filler (40%) exhibits more homogenous distribution in composites compared to that of 10%, 20%, 30% Huntite. Figure 3.12 f-h shows the non-uniform dispersion of magnesium carbonate hydroxy hydrate particles into composite. It is observed that Huntite agglomerates greater than 10µm detected within composite matrix, as depicted in SEM image of Plate 2. Consequently, this non-uniform dispersion led to local agglomeration of Huntite within the polymer (Figure 3.12c). Figure 3.12 i-j shows both Huntite and magnesium carbonate hydroxy hydrate filler exhibits more homogenous distribution in composites compared to that of 10%, 20%, 30%, 40% Huntite and 10%, 20%, 30% magnesium carbonate hydroxy hydrate.

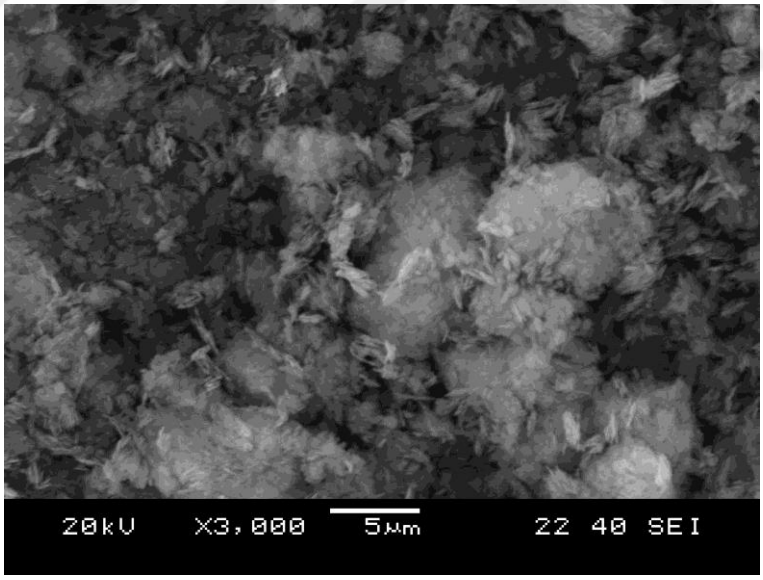


Figure 3.9 SEM Image of Huntite (3000×)

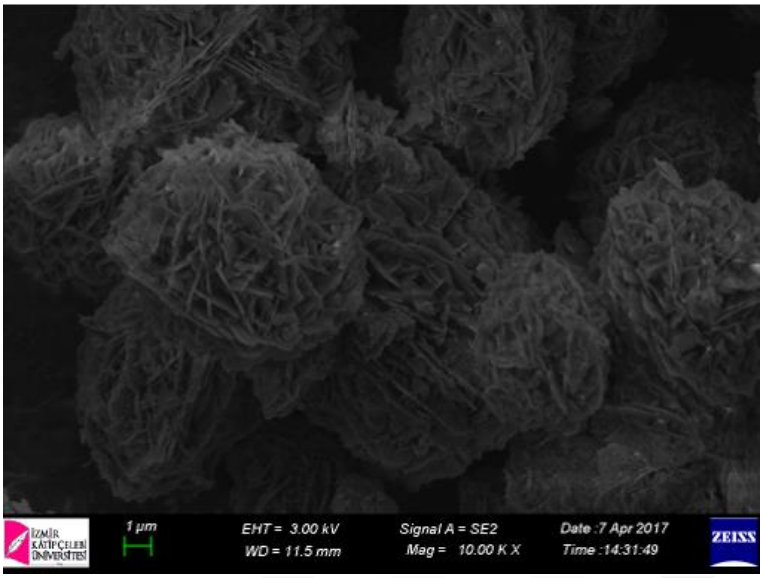


Figure 3.10 SEM Image of Basic magnesium carbonate (1000×)

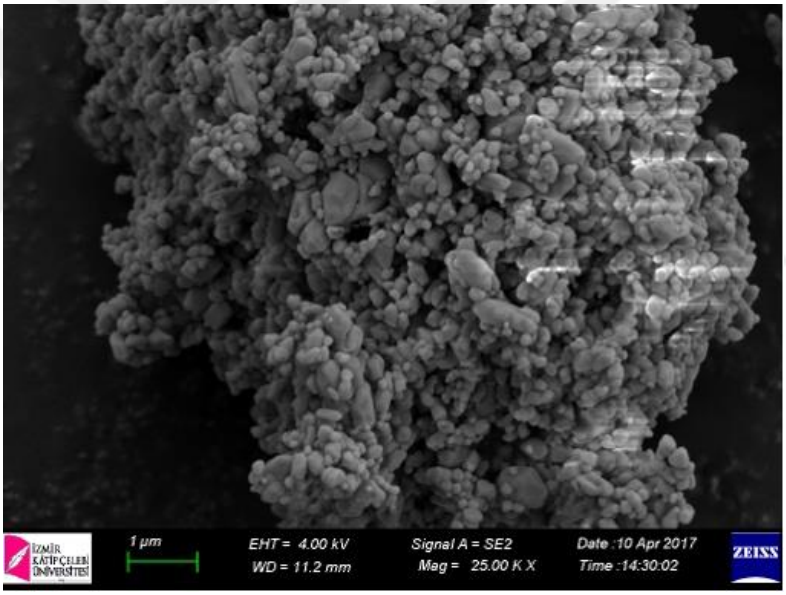


Figure 3.11 SEM Images of Filler26-Barium sulphate ($BaSO_4$) (2500×)

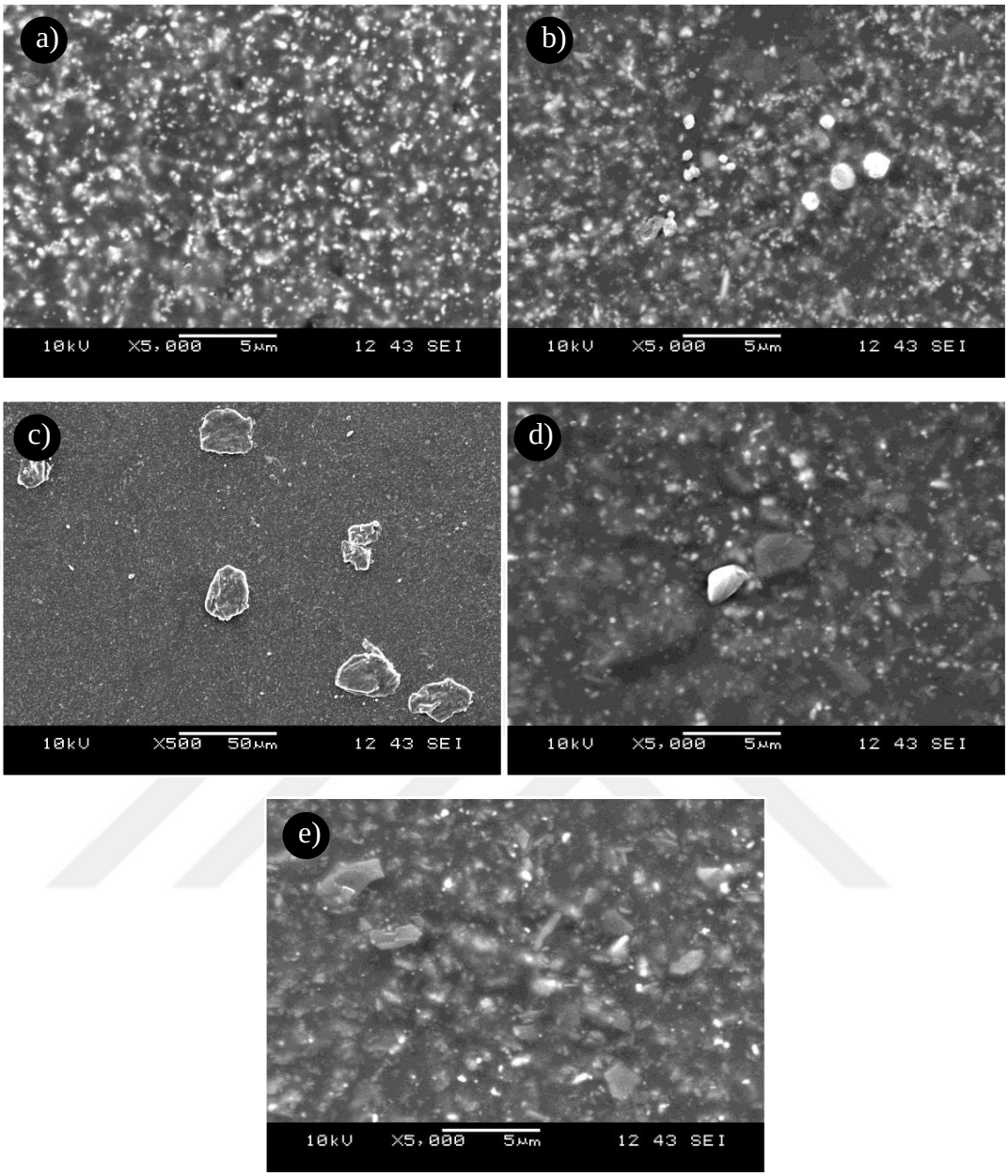


Figure 3.12 SEM images of (a) Plate 0 (5000×), (b) Plate 1 (5000×), (c) Plate 2 (500×) (d) Plate 3 (5000×), (e) Plate 4 (5000×), (f) Plate 5 (10000×), (g) Plate 6 (2500×), (h) Plate 7 (5000×), (i) Plate 8 (2500×), (j) Plate 9 (5000×)

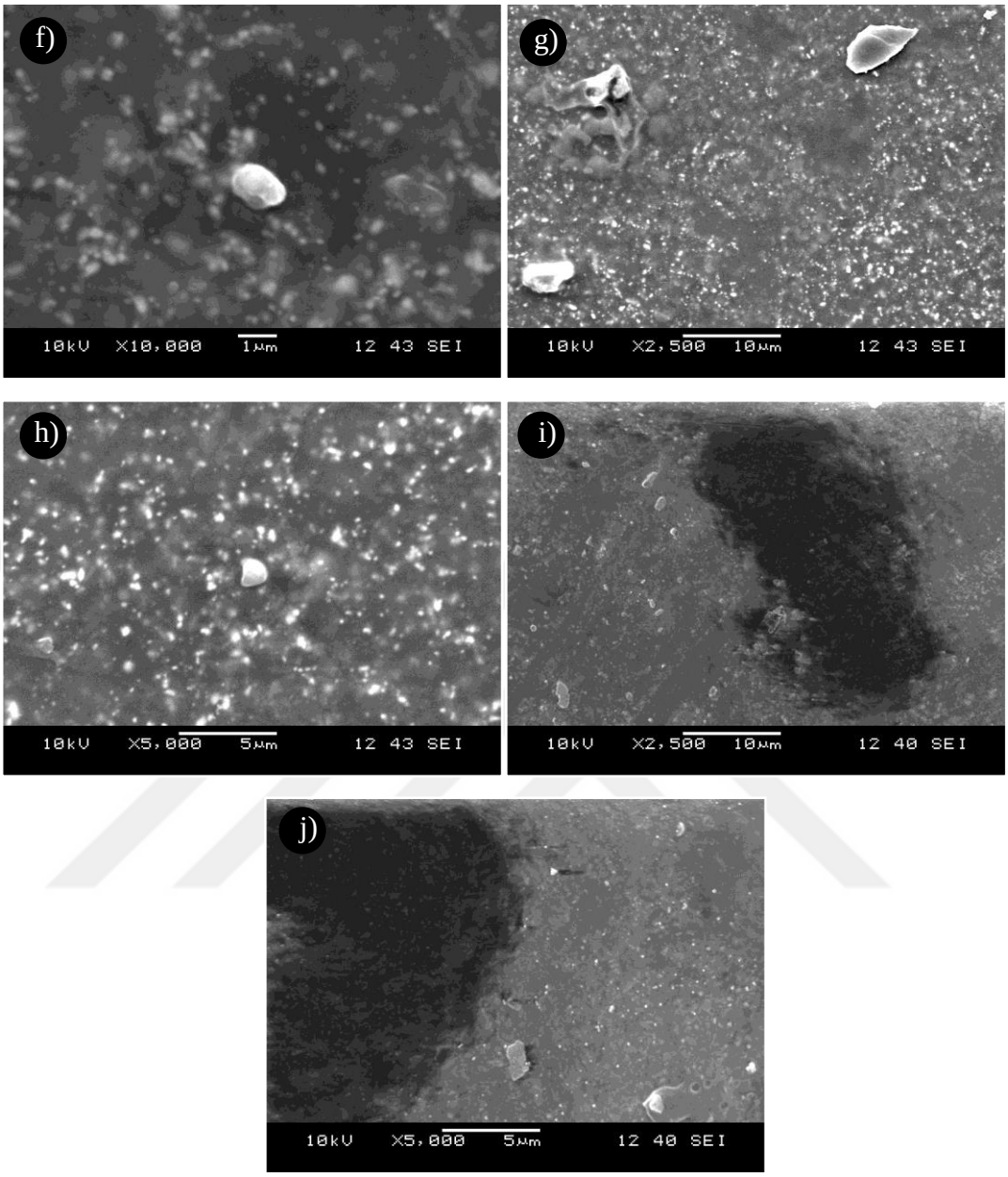


Figure 3.12 SEM images of (a) Plate 0 (5000×), (b) Plate 1 (5000×), (c) Plate 2 (500×) (d) Plate 3 (5000×), (e) Plate 4 (5000×), (f) Plate 5 (10000×), (g) Plate 6 (2500×), (h) Plate 7 (5000×), (i) Plate 8 (2500×), (j) Plate 9 (5000×) (Continued)

3.3 Fourier Transform Infrared Spectroscopy (FTIR) analysis

In Figure 3.13 and 3.14, FTIR spectrum of $BaSO_4$ and MCHH were presented respectively.

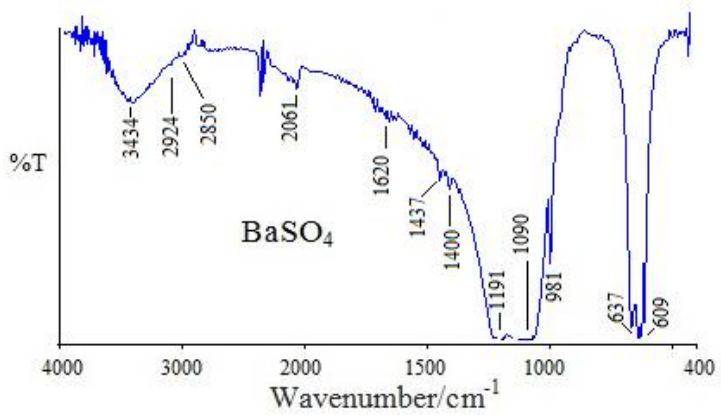


Figure 3.13 FTIR Spectrum of $BaSO_4$

Figure 3.13 shows the FTIR spectrum of the $BaSO_4$. It was well known that the sulfate group has four fundamental vibrational modes attributed to one nondegenerate mode (ν_1), one doubly degenerate mode (ν_2), and two triply degenerate modes (ν_3 and ν_4). In general, the IR spectrum of $BaSO_4$ or Baryte mineral exhibits two intense bands correspond to asymmetric stretching and bending (ν_3 and ν_4), and two weak ones correspond to symmetric stretching and bending ($\nu_1$and ν_2) (Prameena, 2013). In the Figure 3.13, the bands centered at 1090–1191 cm^{-1} and the shoulders at 981 cm^{-1} were assigned to symmetric stretching vibration of SO_4^{2-} group. At 1620 cm^{-1} the stretching vibration ν_3 of SO_4^{2-} group was observed. The bands at 609 and 637 cm^{-1} were attributed to the out-of-plane bending vibration of the SO_4^{2-}(Gupta, 2010; Prameena, 2013). The broad absorption band appeared at 3434 $cm^{-1}$is due to antisymmetric stretching vibrations of H_2O molecules localized on vacant sites of Ba. The band at 2061 cm^{-1} is overtone and a combination of stretching and bending vibrations bands of the sulphur-oxygen (Manam & Das, 2009).

On the other hand, the bands at 2850 and 2924 cm^{-1} could be assigned to the symmetric and asymmetric vibrations of $-CH_2-$ and $-CH_3$ groups. The bands at 1436 and 1400cm^{-1} were ascribed to the scissoring of $-CH_2-$ or the symmetric deformation of the $-CH_3$ group due to the usage of polycarboxylate as a modifier in the preparation of $BaSO_4$ (Saraya & Bakr IM, 2011).

FTIR spectrum of MCHH was presented in Figure 3.14. The O-H vibration gives rise to a sharp band at 3652 cm^{-1}. The bands at 3518 and 3450 cm^{-1} were resulting from water of crystallisation (Botha & Strydom, 1971).

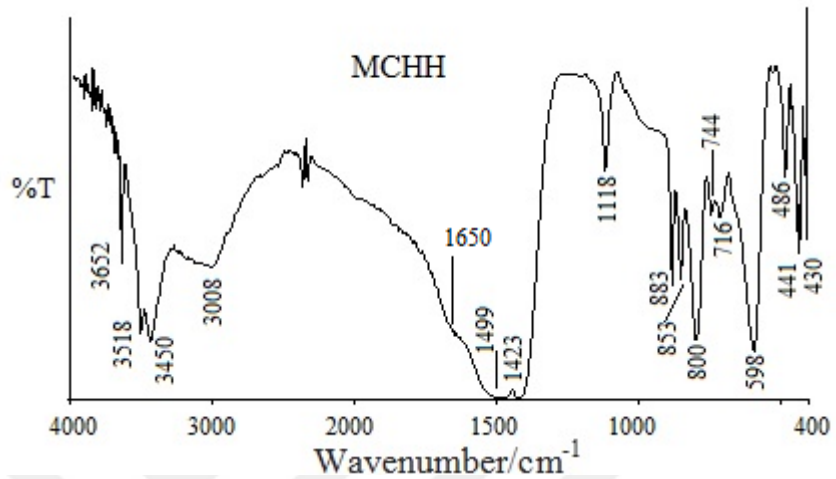


Figure 3.14 FTIR Spectrum of MCHH

The H_2O bending vibration band at 1650 cm^{-1} is very weak and appears as a shoulder on the side of the CO_3^{2-} stretching band (White, 1971). The CO_3^{2-} asymmetric stretching vibrations are observed as a strong band split in two at 1423-1499 cm^{-1}. This is a characteristic of the bicarbonate and shows that the carbonate ion in the MCHH exists as bicarbonate. The three absorption bands at 800 cm^{-1}, 853 and 883 cm^{-1} are assigned to CO_3^{2-} bending vibrations. A band at 1118 cm^{-1} is assigned to the CO_3^{2-} ν_1 symmetric stretching vibration (Sawada et. al., 1978; Choudhari et. al., 1972). Figure 3.15 shows the FTIR spectra of Plates 0-4. The main difference in the spectra was observed in the range of 1600-1400 cm^{-1}. This difference was clear in the spectrum of Plate 4. As can be seen from the spectrum of Plate 0, $-CH_3$ asymmetric bending vibrations were assigned at 1420 cm^{-1}. Asymmetric stretching bands of CO_3^{2-} were observed at 1538 and 1446 cm^{-1} (Kangal & Güney, 2006; Barbieri et. al., 1974). After 40% Huntite was added into composites, the new bands in the spectrum of polyester came about because of asymmetric stretching bands of CO_3^{2-} of Huntite, as presented in Figure 3.15. The band at 1506 cm^{-1} is due to asymmetric stretching bands of CO_3^{2-} of Huntite.

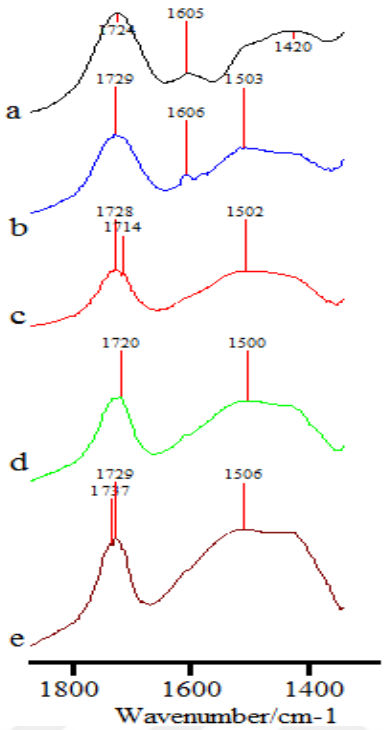


Figure 3.15 FTIR spectra of a) Plate 0 b) Plate 1 c) Plate 2 d) Plate 3 e) Plates 4

3.4 Thermogravimetric Analysis (TGA)

The thermal decomposition of Huntite, Filler (Filler26, $BaSO_4$ or Barite), Magnesium carbonate hydroxide hydrate (MCHH) have been investigated by TGA under nitrogen flow. TG/DTG of the Huntite, Filler (Filler26, $BaSO_4$ or Barite), Magnesium carbonate hydroxide hydrate (MCHH) were presented in Figure 3.16, Figure 3.17 and Figure 3.18 respectively. As can be seen from Figure 3.16, Huntite decomposed through two stages and the TG/DTG data was given in Table 3.1. The first stage occured between 400 and 630 ℃ with a loss of 36.2%, the second stage occured between 630 and 750 ℃ with a further mass loss of 12% and making a total mass loss of 48.2%. Huntite has a total molecular mass of 353 g mol^{-1}. Since it is a carbonate mineral it is likely that its thermal decomposition consists of release of carbon dioxide. Release of three carbon dioxide molecules followed by further release of one carbon dioxide molecule gives calculated mass losses of 37.4% and 12.5%, which is in very close agreement with the measured values. The decomposition reactions were given below;

$$Mg_3Ca(CO_3)_4 \longrightarrow CaCO_3 + 3MgO + 3CO_2(\text{FirstStage}) \quad (3.1)$$

$$CaCO_3 \longrightarrow CaO + CO_2(\text{Second Stage}) \quad (3.2)$$

According to the Figure 3.17 and Table 3.1, it can be said that Filler, Filler26 is composed of mainly $BaSO_4$ and very stable at least 1000℃ as compared with Huntite and MCHH only 1.7% mass loss observed due to impurities. On the other hand, the thermal decomposition of the Magnesium Carbonate Hydroxide Hydrate (MCHH)occurs at three stages. The first stage is related with crystalline water. The second stage is due to decomposition of hydroxide ion, releasing water. The third stage is due to decomposition of carbonate ions associated with Mg.

$$C_4Mg_4O_{12}.H_2MgO_2.xH_2O \longrightarrow C_4Mg_4O_{12}.H_2MgO_2 + xH_2O(\text{First Stage}) \quad (3.3)$$

$$C_4Mg_4O_{12}.H_2MgO_2 \longrightarrow C_4Mg_4O_{12} + MgO + H_2O(\text{Second Stage}) \quad (3.4)$$

$$C_4Mg_4O_{12} \longrightarrow 4MgO + 4CO_2(\text{Third Stage}) \quad (3.5)$$

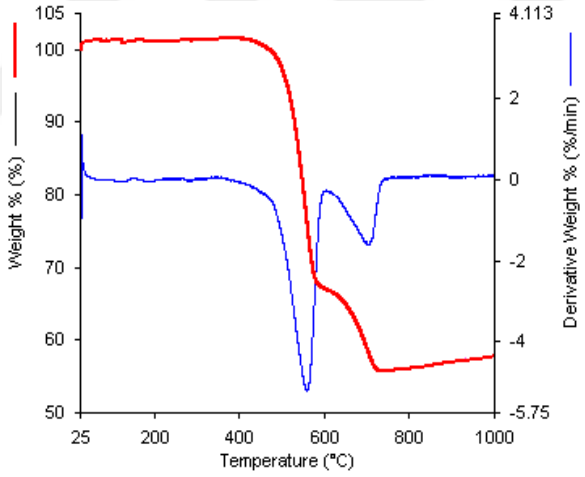


Figure 3.16 TG/DTG profile of Huntite

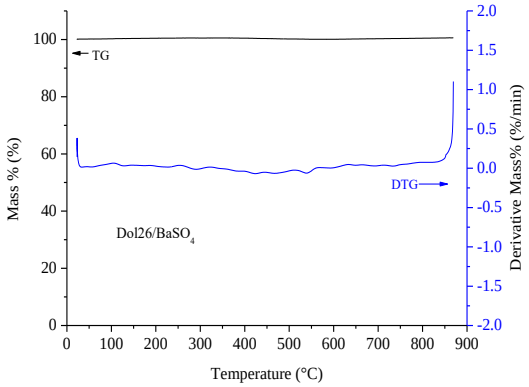


Figure 3.17 TG/DTG profile of Filler26- $BaSO_4$

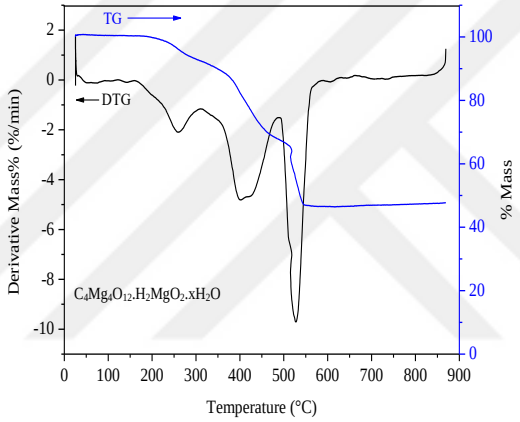


Figure 3.18 TG/DTG profile of MCHH

Table 3.1 TG/DTG Analysis Data of Huntite, $BaSO_4$ and MCHH

Sample	First stage		Second stage		Third stage		Mass % remaining after 1000°C
	T_{max} (°C)	Mass loss %	T_{max} (°C)	Mass loss %	T_{max} (°C)	Mass loss %	
Huntite	558	36.2	705	12.0	-	-	51.8
$BaSO_4$	513	1.7	-	-	-	-	98.3
MCHH	263	8.3	399	24.9	528	19.8	47.0

Thermogravimetric and DTG curves of Epoxy GS 7351, Polyester 4783 and Polyester 6400 that were used in the composites were shown in Figure 3.19 and the data was given in Table 3.2.

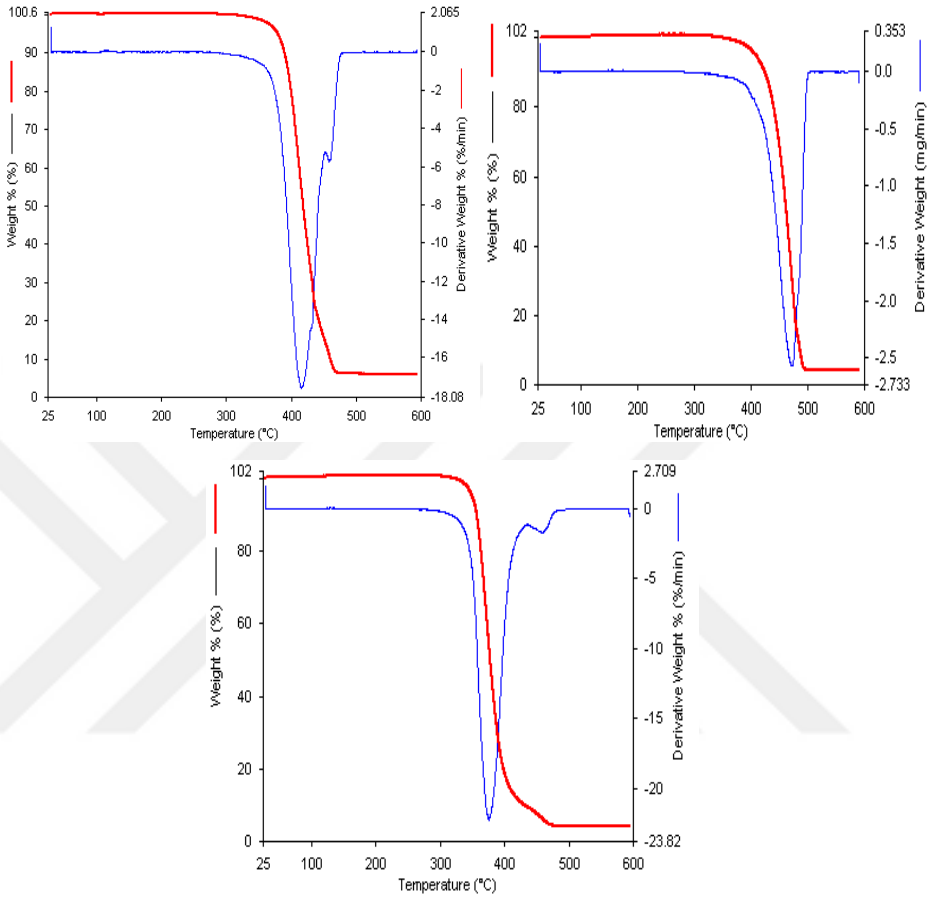


Figure 3.19 Thermogravimetric and DTG curves of Epoxy GS 7351, Polyester 4783 and Polyester 6400

Table 3.2 TG/DTG Data of Epoxy GS 7351, Polyester 4783 and Polyester 6400

Sample	First stage		Second stage		Mass % remaining after 600ºC
	T_{max} (°C)	Mass loss %	T_{max} (°C)	Mass loss %	
Epoxy GS 7351	415	85.3	460	8.6	6
Polyester 4783	472	96.6	-	-	4
Polyester 6400	375	91.3	460	5.5	4

As can be seen from Figure 3.19 and from the data presented in Table 3.2, Polyester precursor that were used in the production of the composites, they were stable till 350°C and decomposed almost totally above 500ºC.

Thermal behaviour of the Plates was also investigated by TGA/DTG. TGA thermogramswere shown in Figure 3.20 and the results were given in Table 3.3.

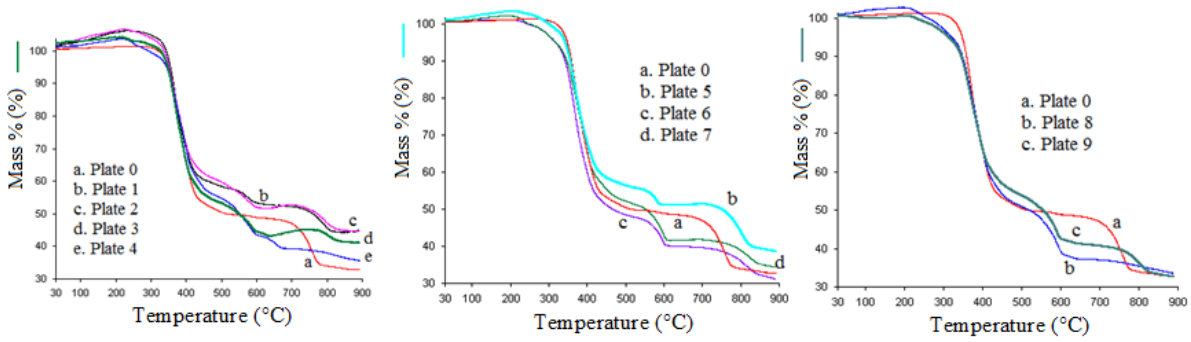


Figure 3.20TGA Thermograms of the Plates

Table 3.3 TGA/DTGdata of the Plates

Sample	First stage		Second stage		Third stage		Fourth stage		Mass % remaining after 900°C
	T_{max} (°C)	Mass loss %	T_{max} (°C)	Mass loss %	T_{max} (°C)	Mass loss %	T_{max} (°C)	Mass loss %	
Plate 0	373	50	586	1	759	16	-	-	33
Plate 1	370	47	575	5	792	8	-	-	40
Plate 2	369	47	594	8	792	8	-	-	37
Plate 3	370	49	595	11	800	4	-	-	36
Plate 4	244	2	397	48	580	13	654	4	33
Plate 5	370	47	579	5	801	13	-	-	35
Plate 6	368	53	592	8	818	9	-	-	30
Plate 7	233	2	390	48	594	10	818	8	32
Plate 8	238	3	394	48	590	14	-	-	35
Plate 9	233	2	368	44	589	13	804	7	33

Plate 0 was chosen as a reference which contains mainly Filler26 as filler. Plate 0 and Plate 4 are comparable. Plate 0 has 43% $BaSO_4$ and Plate 4 has 40% Huntite. The T_{max} (1st step) value decreases from 373 ℃ to 244 ℃ and the mass loss decreases from 50% to 2%. T_{max} (2nd step) temperature is reduced from 586 ℃ to 397 ℃. Mass loss is 48% from 1%. Considering that $BaSO_4$ does not decompose at these temperatures, the deterioration temperature of the material is going up 244 ℃ to 397 ℃, if we do not take into account the practically first 2% loss of the Huntite (which may be due to moisture). As can be seen from Figure 3.20, Plate 4's degradation begins earlier than other Plates except Plate 7, 8 and 9. The order of degradation starting temperature was followed as Plate 4, Plate 3, Plate 2, Plate 1 and Plate 0. The results showed that when 40% Huntite was added (Plate 4), thermal stability in terms of maximum degradation temperature reached a maximum value (397 ^oC) at first stage degradation and when 30% Huntite was added (Plate 3), thermal stability in terms of maximum degradation temperature reached a maximum value (595 ℃) at the second stage degradation. As can be seen from Figure 3.20 c, Plate 8's degradation begins earlier than Plate 9's degradation. The order of degradation starting temperature was followed as Plate 8, Plate 9, and Plate 0. It can be claimed that maximum degradation temperature of composite was improved by adding 20% Huntite into composite.

As can be seen from Figure 3.20 and Table 3.3, it can be said that $C_4Mg_4O_{12}.H_2Mg_2O_2.xH_2O$-containing composites (Plates 5-6-7) and Huntite containing some composites (Plate1, 2 and 3) was not affected by curing process at 200 ℃ but some Huntite containing and both MCHH-Huntite containing composites (Plates 1-2-8-9) was affected by curing process at 200℃. It can be claimed that Plate 3-4 was not affected by curing process because that Huntite filler exhibits more homogenous distribution as compared to in Plates 1-2-5-6-7-8-9. On the other hand, when the thermal stability of Plates 1, 2-3 and Plates 5, 6-7 (ie, samples containing Huntite and MCCH in the same quantities) are compared, only Plate 7 (30% MCHH) is observed to differ. Plate 4 (%40 Huntite) and Plate 7 (%30 MCHH) were better than the others in terms of thermal stability.

3.5 Differential Thermal Analysis

Exothermic and endothermic reactions between the components of the reactants are significant in the evaluation of flame retardancy. DTA analyses are carried out to correlate interactions between Huntite, MCHH and polymer composites. DTA analyses are performed in the temperature range of 25-600 ºC at a heating rate of 10 ºC min^{-1} in nitrogen gas atmosphere.

Huntite and Magnesium carbonate hydroxy hydrate have $Mg_3Ca(CO_3)_4$ and $C_4Mg_4O_{12}.H_2Mg_2O_2.xH_2O$ chemical formulas respectively. Because of these structures, decomposition occurred in these minerals at temperatures between 25 ºC and 600 ºC. DTA results were given in Table 3.4. The thermal phenomena of Plate 0 starts at 440 ºC and ends at 457 ºC and then heat absoption is -1568 J, corresponding to the combustion of carbon based materials containing in pure powder coating. The thermal phenomena of Plate 1 (contains %10 Huntite) starts at 455 ºC and ends at 464 ºC then heat absoption is -1739 J. The thermal phenomena of Plate 2 (contains %20 Huntite) starts at 437 ºC and ends at 464 ºC and then heat absoption is -1378 J. The thermal phenomena of Plate 3 (contains %30 Huntite) starts at 449 ºC and ends at 477 ºC and then heat absoption is -1330 J. The thermal phenomena of Plate 4 (contains %40 Huntite) starts at 454 ºC and ends at 475 ºC and then heat absoption is -1480 J. The first thermal phenomena of Plate 5 (contains %10 Magnesium carbonate hydroxy hydrate) starts at 446ºC and ends at 463ºC and then heat absoption is -1267 J. The second thermal behavior of Plate 5 starts at 507 ºC and ends at 530 ºC and then heat absoption is -221 J. The thermal phenomena of Plate 6 (contains %20 MCHH) starts at 446 ºC and ends at 475 ºC and then heat releases at -1145 J. The second thermal behavior of Plate 6 starts at 511 ºC and ends at 541 ºC and then heat absoption is -408 J. The thermal phenomena of Plate 7 (contains %30MCHH) starts at 433ºC and ends at 468ºC and then heat absoption is -1140 J. The second thermal behavior of Plate 7 starts at 507ºC and ends at 535 ºC and then heat absoption is-535 J. The thermal phenomena of Plate 8 (contains %20 Huntite and %20 MCHH) starts at 434 ºC and ends at 473 ºC and then heat absoption is -1147 J. The second thermal behavior of Plate 8 starts at 516 ºC and ends at 541 ºC and then heat absoption is -262 J. The thermal phenomena of Plate 9 (contains %12.6 Huntite and %12.6 MCHH) starts at

433 ºC and ends at 468 ºC and then heat absoption is -1109 J. The second thermal behavior of Plate 9 starts at 498 ºC and ends at 526 ºC and then heat absoption is -335J.

Heat release reduces obviously during most of the heating process due to endothermic reactions of Huntite/Magnesium carbonate hydroxy hydrate, especially between 400 ℃ to 500 ℃ (except plate 1).

Addition of Huntite and MCHH to the polymer matrix can both increase the peak decomposition temperature.

Table 3.4 Results of Differential Thermal Analysis for Plates 0-9.

Sample	First stage				Second stage				Mass % remaining after 590℃
	Onset T(℃)	End T(℃)	Peak T (℃)	ΔH J/g	Onset T(℃)	End T(℃)	Peak T (℃)	ΔH J/g	
Plate 0	440	457	452	-1568	-	-	-	-	33.0
Plate 1	455	464	461	-1739	-	-	-	-	27.1
Plate 2	437	464	458	-1378	-	-	-	-	27.1
Plate 3	449	477	465	-1330	-	-	-	-	23.4
Plate 4	454	475	460	-1480	-	-	-	-	26.8
Plate 5	446	463	457	-1267	507	530	521	-221	33.8
Plate 6	446	475	465	-1145	511	541	529	-408	33.0
Plate 7	433	468	457	-1140	507	535	525	-535	26.1
Plate 8	434	473	459	-1147	516	541	530	-262	10.6
Plate 9	433	468	459	-1109	498	536	526	-335	19.5

3.6 Differential Scanning Calorimetric (DSC) Analysis

DSC curves of the uncured plate (UCP) samples of UCP 0 and UCP 4 were given below as Figure 3.21. DSC data was also summarized on Table 3.5.

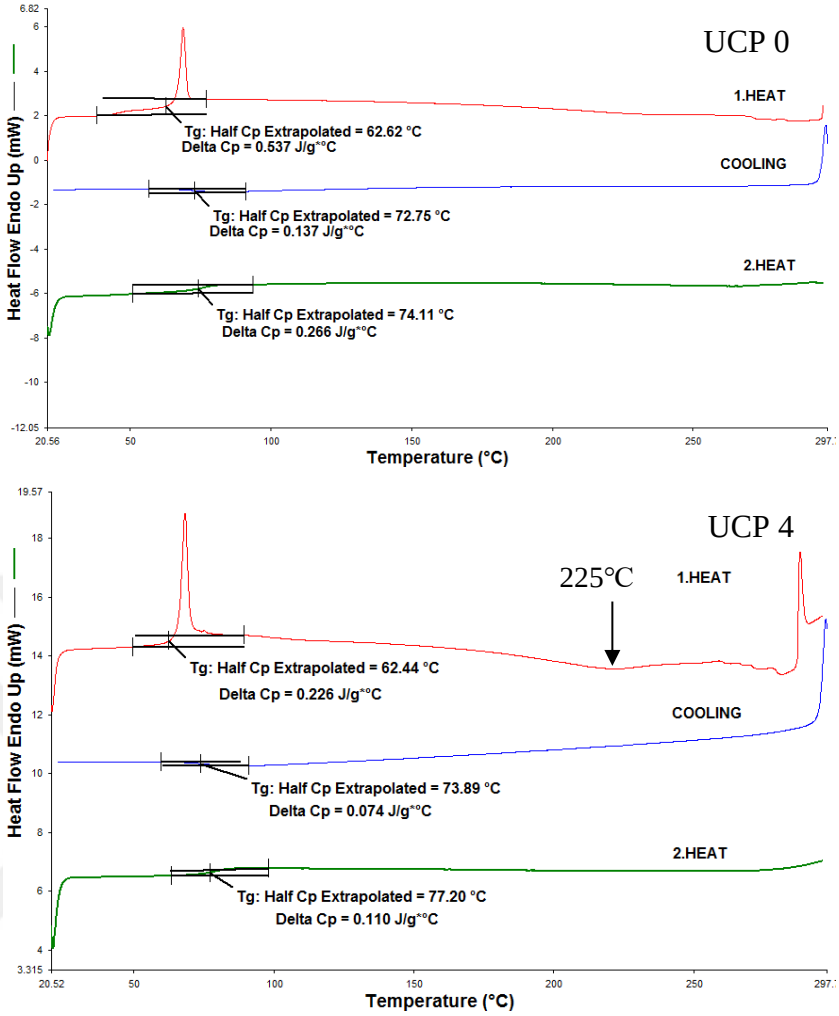


Figure 3.21 DSC curves of UCP 0 and UCP 4

Table 3.5 DSC data of the UCP 0-7 samples (After Second Heating Period)

Sample	Flame retardants		T_g (°C) 1.Heating-Cooling-2.Heating			ΔCp (J/g°C)	ΔH (J/g)
	Huntite	MCHH					
UCP 0	-	-	62.6;	72.8;	74.1	0.266	19.71
UCP 1	10	-	63.7;	73.6;	74.2	0.252	18.70
UCP 2	20	-	63.4;	71.5;	73.3	0.215	15.77
UCP 3	30	-	62.5;	72.2;	74.5	0.171	12.74
UCP 4	40	-	62.4;	73.9;	77.2	0.110	8.49
UCP 5	-	10	64.8;	72.2;	74.6	0.186	13.87
UCP 6	-	20	65.1;	66.8;	73.8	0.192	14.17
UCP 7	-	30	65.3;	78.1;	80.3	0.194	15.58

It has been reported that the surface characteristics of composites and fibrous reinforcement influence the curing behavior of thermosetting resins (Choudhari & Vaidya, 1972).

In order to determine whether Huntite or/and MCHH affects the curing behavior of powder coatings, DSC analysis in heat-cool-heat mode (so curing could proceed during heating part of the cycle) was carried out. The T_g values of UCP 0-8 are 74.1, 74.2, 73.3, 74.5, 77.2, 74.6, 73.8 and 80.3 °C, respectively. As can be seen from DSC curve of polyester, one endotherm from first heating run were observed. T_g, ΔH, ΔCp values of UCP 0-7 (First heating) are given in Table 6. The glass transition temperature (T_g) increases with increasing powder coating/MCHH composites ratio (UCP 5-7). The glass transition temperature (T_g) increasing show no correlation behaviour with increasing powder coating/Huntite composites ratio (UCP 1-4). The increase in the glass transition temperature can be explained by the interaction of the polymeric matrix with Huntite and MCHH, hindering the molecular mobility. As shown in Table 3.5, the ΔH based on UCP 1-8 was lower than that of the UCP 0. This means that the Huntite andMCHH in the hybrid network structure absorb heat and act as a heat sink in the composites. The ΔH of the powder coating/Huntite composites (UCP 1-4) was lower than that of the powder coating/MCHH composites (UCP 5-7) under the same conditions.

3.7 UL94 Flammability Test

The effect of the flame retardants on the UL94 vertical burning tests of composites were presented in Table 3.6. According to their UL94 test data, all the systems showed V0 rating. LOI test method was performed and observed no burning. Surface roughness was influenced by flame due to flame retardant content of coatings. After test, images of samples were shown in Figure 3.22.

Table 3.6 Formulations and Flame Retardancy for the coatings

Sample	Average Burn time (t_1)	UL-94 rating	Smoke
Plate 0	7	V-0	No
Plate 1	9	V-0	No
Plate 2	7	V-0	No
Plate 3	6	V-0	No
Plate 4	7	V-0	No
Plate 5	7	V-0	No
Plate 6	6	V-0	No
Plate 7	8	V-0	No
Plate 8	6	V-0	No
Plate 9	6	V-0	No

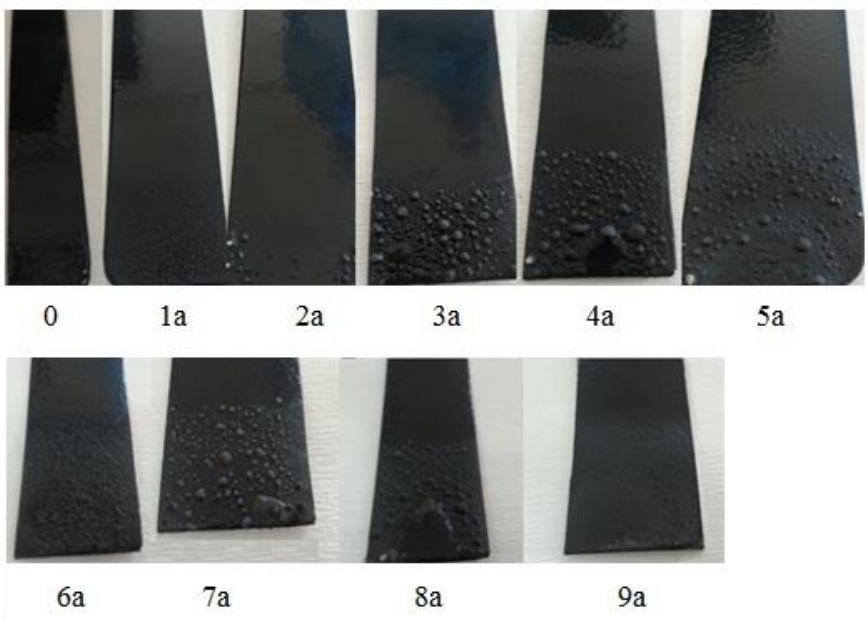


Figure 3.22 UL94 Vertical Flammability Test Images of samples

The release of water vapour creates a foamed structure which increases the insulation effect on the polymer. The bubbles were observed increasingly from Plate 3 to Plate 8. This may be due to the fact that water vapour and carbon dioxide formed in the decomposition of MCHH and Huntite (Plate 7 and 8 seen in Figure 3.22). They were released into the flame when degradation of the polymer reduced its viscosity to

the degree at which the bubbles could move through the polymer or the degradation of polymer caused the bubbles near the surface to burst. This was not observed well in Plate 9.

LOI experiments were also carried out. It can be seen that the pure polymeric matrix is highly combustible with the LOI value of 20.0%. The LOI value of the Plate 0 was increased to 30.3%. The flame retardancy of the Plates 1-4 gradually increased with the improvement of the Huntite. The Plate 1 can successfully pass UL94 observed in V-0 flammability rating and the LOI value is as high as 31.4% and reached to 33.2% for Plate 4 which had 40% Huntite. On the other hand, interesting results were the case of Plates 7, 8 and 9. This means that Plate 7 (%13$BaSO_4$, %30 MCHH), Plate 8 (%3 $BaSO_4$, %20 Huntite and %20 MCHH), and Plate 9 (%17.8 $BaSO_4$, %12.6 Huntite and %12.6 MCHH) showed almost same UL94 and LOI behaviour of around %35 of O_2.

CHAPTER FOUR
CONCLUSIONS

In this Thesis, flame retardant properties of composites were investigated and developed in some respect. In this context, the composite materials were obtained by adding different amounts of halogen-free, environmental friendly retardants such as Huntite and Magnesium carbonate hydroxy hydrate (MCHH) to powder coating material. UL94 and LOI test results were perfect. The best results were obtained in the Huntite reinforced composite coatings. The usage of Huntite instead of filling material can also have several advantages by enhancing the properties ofcomposites, such as mechanical properties, flame retardancy, barrier properties and reducing the cost of filling material. From the flame retardancy properties of Huntite/hydromagnesite mineral in powder coatings as discussed in this work, it can be considered that flame retardants help to increase safety in virtually every area of human existence.

Plate 4 and Plates 7, 8 and 9 showed similar behavior. It may be said that Huntite is not a very effective fire retardant when it is used alone. This argument was also discussed before in the reports Kirschbaum et al. (Kirschbaum, 1998; Kirschbaum, 2001). It should be used together with $BaSO_4$ and MCHH, but not more than totaly %40 as filler content.

As a result, the fire retardant action of mixtures of $BaSO_4$, Huntite and MCHH comes from the combined actions at least these two minerals together. Huntite and MCHH are certainly not the inert diluents that have been claimed by some in the past. This study has provided a step forward in the understanding of the fire retardant mechanisms of Huntite and MCHH. Huntite and MCHH mixtures would be well suited to use in this polymer matrix. Due to limitations with the equipments, smoke measurements were not possible. A study related with the contribution of both Huntite and MCHH on smoke production should be carried out in future.

REFERENCES

Akzo Nobel. (1999). *Complete Guide to Powder Coatings*, Issue 1, November 1-10.

Alexander, B. M., & Charles, A. W. (2007). *Flame retardant polymer nanocomposites.* New Jersey: Wiley.

Barbieri, M., Calderoni, G., Cortesi, C., & Fornaseri, M. (1974). Huntite: a mineral used in antiquity. *Archaeometry, 16*, 211–220.

Beard, A. (2007). Flame retardants - Frequently Asked Questions. *The European Flame Retardants Association (EFRA).* p.37.www.flameretardants.eu.

Beck, C. W. (1950) Differential thermal analysis curves of carbonate minerals. *American Mineralogist, 35*, 985-1013.

Bolger, R. (1996). Flame retardant minerals bromine issue smoulders on. *Industrial Minerals*, 29-39.

Botha, A., & Strydom, C. A. (2003). DTA and FT-IR analysis of the rehydration of basic magnesium carbonate. *Journal of Thermal Analysis and Calorimetry,71*, 987-995.

Bourbigot, S., & LeBras, M. (2004). Flame retardant plastics. In Troitzsch, J. (Ed.). *Plastics flammability handbook* (133-172). Munich: Hanser.

Brett, N. H., MacKenzie, K. J. D., & Sharp, J. H. (1970). The thermal decomposition of hydrous layer silicates and their related hydroxides. *Quarterly Reviews of the Chemical Society,24*, 185-207.

Charles, A. W., & Alexander, B. M. (2009). *Fire retardancy of polymeric materials.* Parkway: CRC Press.

Choudhari, B. P., Vaidya, M. C., & Datar, D.S. (1972). Physicochemical studies on basic magnesium carbonates. *Indian Journal of Chemistry, 10*, 731-733.

Cullis, C. F., & Hirschler, M. M. (1981). *The combustion of organic polymers*. London: Oxford University Press.

Dana, J., & Ford, W. (1929). *Dana's Manual of Mineralogy For the Student of Elementary Mineralogy, the Mining Engineer, the Geologist, the Prospector, the Collector, etc*, (14th ed.) NewYork, NY, USA: John Wiley & Sons.

Dastoori, K., & Makin, B. (2001). Measurement of thickness and adhesive properties of electrostatic powder coatings for standard and modified powder coating guns. *Journal of Electrostatics, 51-52,* 545-551.

Demirel, M., Pamuk, V., & Dilsiz, N. (2010). Investigation of flame retardancy and physical-mechanical properties of Zinc Borate/Boric Acid Polyester Composites. *Journal of Applied Polymer Science, 115*(5), 2550-2555.

Dufton, P.W., (2003). *Flame retardants for plastics market report.* Birmingham: Rapra Technology Limited.

Durin-France, A., Ferry, L., Cuesta, J. L., & Crespy, A. (2000). Magnesium hydroxide/zinc borate/talc compositions as flame-retardants in EVA copolymer. *Polymer International, 49* (10), 1101-1105.

Ellis, B. (1993). (Ed.). *In chemistry and technology of epoxy resin*. London: Blackie Academic and Professional.

Faust, G. T. (1953). Huntite, $MgBCa(CO_3)_4$, a new mineral. *American Mineralogist, 38*, 4-24.

Fink, U. (2004). The market situation. In: Troitzsch, J. (Ed.). *Plastics flammability handbook* (8-32). Munich, Germany: Carl Hanser Verlag.

Fire triangle. (n. d.). Retrieved December 1, 2011, from http://firextinguishing.blogspot.com/search/label/Introduction

Fuentes, G., Almandoz, E., & Pierrugues, R. (2010). High temperature tribological characterization of TiAlSiN coatings produced by cathodic arc evaporation. *Surface and Coatings Technology*, *205*, 1368-1373.

Georgiades, G. N., Larsson, B. J., & Pust, C. (1996). Huntite-hydromagnesite production and applications. *In: Proceedings 12th Industrial Minerals Congress*, 57-60.

Georlette, P., Simons, J., & Costa, L. (2000). Halogen-containing fire-retardant compounds. In Grand, A. F., & Wilkie, C. A., (Eds.). *Fire Retardancy of Polymeric Materials* (245-284). New York: Marcel Dekker.

Green, J. (1983). Calcination of precipitated $Mg(OH)_2$ to active MgO in the production of refractory and chemical grade MgO. *Journal of Materials Science*, *18*(3), 637-651.

Gupta, A., Singh, P., & Shivakumara, C. (2010). Synthesis of $BaSO_4$ nanoparticles by precipitation method using sodium hexa metaphosphate as a stabilizer. *Solid State Communications*, *150*(9-10*)*, 386–388.

Hancock, M., & Rothon, R. N. (2003). Principle types of particulate fillers. In Rothon, R. N., (Ed.). *Particulate filled polymer composites* (53-100). Shrewsbury: Rapra Technology Ltd.

Hanor, J. S. (2000). Barite-celestine geochemistry and environments of formation, *Reviews in Mineralogy and Geochemistry*, *40*, 193–275.

Henrist, C., Mathieua, J. P., Vogelsb, C., Rulmonta A., & Clootsa R. (2003). Morphological study of magnesium hydroxide nanoparticles precipitated in dilute aqueous solution. *Journal of Crystal Growth*, *249*, 321-330.

Hollingbery, L. A., & Hull, T. R. (2010). The fire retardant behaviour of Huntite and hydromagnesite- A review. *Polymer Degradation and Stability, 95*, 2213 -2225.

Hollingbery, L. A., & Hull, T. R. (2010). The thermal decomposition of Huntite and hydromagnesite—A review. *Thermochimica Acta*, *509*, 1-11.

Horn, W. E. (2000). Inorganic hydroxides and hydroxycarbonates: Their function and use as flame-retardant additives. In Grand, A. F., & Wilkie, C. A., (Eds.). *Fire retardancy of polymeric materials* (285-352). New York: Marcel Dekker.

Hornsby, P.R., & Watson, C.L. (1986). Magnesium hydroxide – a combined flame retardant and smoke suppressant filler for thermoplastics. *Plastic Rubber Processing and Applications, 6,* 169–175.

Hornsby, P.R., & Watson, C.L. (1989). Mechanism of smoke suppression and fire retardancy in polymers containing magnesium hydroxide filler. *Plastic Rubber Processing and Applications,11*, 45–51.

Hornsby, P. R., & Watson, C. L. (1990). A study of the mechanism of flame retardanceand smoke suppression in polymers filled with magnesium hydroxide. *Polymer Degradation and Stability, 30*, 73–87.

Hull, R. T. (2016). The Development of Sustainable Fire Retardant Materials. *J Materials China, Online Journal,* (5), 6-10.

Innes, J. D. (1996). Flame retardants and their market applications. Flame retardants-101: basic dynamics, past efforts create future opportunities. *Fire Retardant Chemicals Associations: Baltimor,* 61-69.

Kandelbauer, A., Tondi, G., & Goodman, S. H. (2013). *Handbook of thermoset plastics: 6. unsaturated polyesters and vinyl esters.* Amsterdam: Elsevier Inc. Chapters.

Kandola, B. K. (2008). An Overview of Flame Retardancy. *Proceedings: Flame Retardancy and Flammability of Polymers and Textiles, University of Leeds*.

Kangal, O., & Güney, A. (2006). A new industrial mineral: Huntite and its recovery. *Minerals Engineering, 19*, 376–378.

Kim, S. (2003). Flame retardancy and smoke suppression of magnesium hydroxide filled polyethylene. *Journal of Polymer Science Part B: Polymer Physics, 41*(9), 936-944.

Kirschbaum, G. (2001). Minerals on fire, Flame retardants look to mineral solutions. *3rd Minerals in Compoundings Conference, IMIL-AMI Joint Conference.* 8-10 April 2001.

Kirschbaum, G. (2001). Minerals on fire: flame retardants look to mineral solutions. *Industrial Minerals,* 61-67.

Kirschbaum, G. S. (1998). *Huntite/hydromagnesite-mineral flame retardants as alternative and complement to metal hydroxides*. In: Proceedings flame retardants '98. London, 151-161.

Kleber, W., & Lang, A. (1997). Triboelectrically charged powder coatings generated by running through holes and slits. *Journal of Electrostatics, 40-41*, 237-240.

Langfeld, K., Wilke, A., Sut, A., Greiser, S., Ulmer, B., Andrievici, V., & Schartel, B. (2015). Halogen-free fire retardant styrene–ethylene–butylene–styrene-based thermoplastic elastomers using synergistic aluminum diethylphosphinate–based combinations. *Journal of Fire Sciences, 33*(2), 157-177.

Laoutid, F., Bonnaud, L., Alexandre, M., Lopez-Cuesta, J. M., & Dubois, P. (2009). New prospects in flame retardant polymer materials from fundamentals to nanocomposites. *Materials Science and Engineering, 63*, 100-125.

Laoutid, F., Ferry, L., Leroy, E., & Lopez Cuesta, J.M. (2006). Intumescent mineral fire retardant systems in ethylene–vinyl acetate copolymer: Effect of silica particles on char cohesion. *Polymer Degradation and Stability*, *91*(9), 2140-2145.

Lewin, M., & Weil, E. D. (2001). Mechanisms and modes of action in flame retardancy of polymers. In Horrocks, A. R., Price, D. (Eds.). *Fire retardant materials* (31-68). Cambridge, UK: Woodhead Publishing.

Lu, S., & Hamerton, I. (2002). Recent developments in the chemistry of halogen-free flame retardant polymers. *Progress in Polymer Science*, *27*, 1661-1712.

Manam, J., & Das, S. (2009). Thermally stimulated luminescence studies of undoped, Cu and Mn doped $BaSO_4$ compounds. *Indian Journal of Pure and Applied Physics*, *47*(6), 435–438.

Mazumder, M. K., & Wankum, D. L., (1997). Influence of powder properties on the performance of electrostatic coating process. *Journal of Electrostatics*, *40-41*, 369-374.

Mirabedini, S., & Thompson, G. (2003). Corrosion performance of powder coated Al using EIS. *Progress in Organic Coatings*, *46*,112-120.

Mureinik, R. J. (1997). *Flame retardants, Minerals' growth in plastics*. Euromin'97, 8-10 June 1997, Barcelona, an IMIL Conference.

Nagaraja, B. M., Abimanyu, H., Jung, K. D. & Yoo, K. S. (2007). Preparation of mesostructured barium sulfate with high surface area by dispersion method and its characterization. *Journal of Colloid and Interface Science, 316*, 645-651.

Nelson, G. L. (1994). *The future of fire retardant materials: Applications and regulations.* FRCA: Williamsburg, Virginia.

Ozao, R., & Otsuka, R. (1985). Thermoanalytical investigation of Huntite. *Thermochima Acta*, *86*, 45-58.

Padeste, C., Oswald, H. R., & Reller, A. (1991). The thermal behaviour of pure and nickel-doped hydromagnesite in different atmospheres. *Materials Research Bulletin, 26*, 1263- 1268.

Patel, P., Hull, T. R., McCabe, R. W., Flath, D., Grasmeder, J., & Percy, M. (2010). Mechanism of thermal decomposition of poly (ether ether ketone) (PEEK) from a review of decomposition studies. *Polymer Degradation and Stability*, *95*, 709–718.

Powder coating. (n. d.). Retrieved March 8, 2017, from https://en.wikipedia.org/wiki/Powder_coating.

Prameena, B., Anbalagan, G., Sangeetha, V., Gunasekaran, S., & Ramkumaar G. R., (2013). Behaviour of Indian natural baryte mineral. *International Journal of Chemical Technology and Research, 5*, 1, 220–231.

Ramaswamy, R., Vimalathithan, M., & Ponnusamy, V. (2011). Preparation of barium sulphate nanocrystals in ethanol— water mixed solvents. *Journal of Ceramic Processing Research, 12*(2), 173–175.

Rothon, R. N. (2003). Effects of particulate fillers on flame retardant properties of composites. In: R. N. Rothon, (Ed.). *Particulate Filled Polymer Composites. pp.* 263-302, Shrewsbury, UK: Rapra Technology Ltd.

Rothon, R. N., & Hornsby, P. R. (1996). Flame retardant effects of magnesium hydroxide. *Polymer Degradation and Stability,54*(2−3),383-385.

Salah, N., Habib, S. S., Khan, Z. H., Al-Hamedi, S., & Lochab, S. P. (2009). Nanoparticles of $BaSO_4$: Eu for heavy-dose measurements. *Journal of Luminescence, 129*, 192-196.

Saraya, M. El-S. I., & Bakr, I. M. (2011). Synthesis of $BaSO_4$ nanoparticles by precipitation method using polycarboxylate as a modifier. *American Journal of Nanotechnology*, *2*, 1, 106-111.

Sawada, Y., Uematsu, K., Mizutani, N., & Kato, M. (1978a). Thermal decomposition of hydromagnesite $4MgCO_3.Mg(OH)_2.4H_2O$. *Journal of Inorganic and Nuclear Chemistry*, *40*, 979, 82.

Sawada, Y., Uematsu, K., Mizutani, N., & Kato, M. (1978b). Thermal decomposition of hydromagnesite $4MgCO_3$-$Mg(OH)_2$-$4H_2O$ under different partial pressures of carbon dioxide. *Thermochimica Acta, 27*, 45-59.

Sawada, Y., Yamaguchi, J., Sakurai, O., Uematsu, K., Mizutani, N., & Kato, M. (1979a). Thermal decomposition of basic magnesium carbonates under high-pressure gas atmospheres. *Thermochimica Acta, 32*, 277- 291.

Sawada, Y., Yamaguchi, J., Sakurai, O., Uematsu, K., Mizutani, N., & Kato, M. (1979b). Thermogravimetric study on the decomposition of hydromagnesite $4MgCO_3.Mg(OH)_2$. $4H_2O$. *Thermochimica Acta, 33*, 127 - 40.

Sawada, Y., Yamaguchi, J., Sakurai, O., Uematsu, K., Mizutani, N., & Kato, M. (1979c). Isothermal differential scanning calorimetry on an exothermic phenomenon during thermal decomposition of hydromagnesite $4MgCO_3.Mg(OH)_2.4H_2O$. *Thermochimica Acta*, *34*, 233-237.

Shen, Y., Li, C., Zhu, X., Xie, A., Qiu, L., & Zhu, J. (2007). Study on the preparation and formation mechanism of barium sulphate nanoparticles modified by different organic acids. *Journal of Chemical Sciences*, *119*(4), 319–324.

Todor, D. N. (1976). *Thermal analysis of minerals*. Kent, England: Abacus Press.

Troitzsch, J. H. (1988). New trends in the use of halogenated flame retardants in Germany. InR.C. Kidder, (Ed.). *Handbook of flame retardant chemicals and fire testing services*. Pennsylvania, USA: Technomic Publishing Company, Inc.

Unsworth, J., Lunn, B.A., & Innis, P.C. (1993). X-ray attenuation properties of electrically insulating barytes/epoxy composites. *Journal of Materials Science Letters, 12*(3), 132-134.

Vojta, Š., Bečanová, J., Melymuk, L., Komprdová, K., Kohoutek, J., Kukučka, P., & Klánová, J. (2017). Screening for halogenated flame retardants in European consumer products, building materials and wastes. *Chemosphere, 168*, 457-466.

Vogelsberger, W., & Jochen Schmidt, J. (2011). Studies of the solubility of $BaSO_4$ nanoparticles in water: Kinetic size effect, solubility product, and ınfluence of microporosity**.** *The Journal of Physical Chemistry C, 115*, 1388–1397.

Weber, M. (1999). Mineral flame retardants, overview & future trends. *Euromin'99, European Minerals & Markets, Nice, IMIL Conference.*

Weil, E. D. (2000). Synergists, adjuvants, and antagonists in flame-retardant systems. In Grand, A. F., & Wilkie, C. A., (Eds.). *Fire retardancy of polymeric materials* (115-145). New York: Marcel Dekker.

Weil, E. D., & Levchik S.V. (2008). flame retardants in commercial use or development for polyolefins. *Journal of Fire Sciences*, *26*, 5-43.

Weil, E. D., Levchik, S., & Moy, P. (2006). Flame and smoke retardants in vinyl chloride polymers - commercial usage and current developments. *Journal of Fire Sciences*, *24*, 211-236.

Weil, E.D. (1999). Synergists, adjuvants and antagonists in flame retardant systems, in: A.F. Grand and C.A. Wilkie, Eds., *Fire Retardancy of Polymeric Materials*. New York: Marcel Dekker, 115-145.

Weil, E.D., Lewin, M., & Rao, D. (2004). A search for an interactive flame retardant system for ethylene-vinyl acetate, in: *Proceedings of the 15th Conference on Recent Advances in Flame Retardancy of Polymeric Materials,* Stamford, Connecticut.

White, W. B. (1971). Infrared characterization of water and hydroxyl ion in the basic magnesium carbonate minerals. *American Mineralogist, 56*, 46-53.

Yıldırım, S. (2013). *Production and ındustrial application of nanostructured flame retardant reinforced composite materials.* Msc Thesis. Dokuz Eylul University, Izmir.

Yılmaz, A. H., & Çelik, E. (2010). Use of Huntite/hydromagnesite mineral in plastic materials as a flame retardant. *Polymer Composites, 31*, 1692-1700.

Yılmaz, A. H. (2007). *Use of Huntite and hydromagnesite mineral in plastic materials as a flame retardant.* Msc Thesis. Dokuz Eylul University, Izmir.